Theoretical and Experimental Studies of Seafloor Backscatter

Author: Maria Desamparados Torres Medina[1, 2]

Directors: Iain Michael Parnum[3, 4], Alexander Gavrilov[3, 5]

Co-director: Víctor Espinosa Roselló[1, 6]

[1]Universitat Politècnica de València, Escola Politecnica Superior de Gandia, València, Spain, matorme@epsg.upv.es[2], vespinos@fis.upv.es[6]

Centre for Marine Science and Technology, Curtin University of Technology, Perth, Western Australia, Australia, i.parnum@cmst.curtin.edu.au[4], a.gavrilov@cmst.curtin.edu.au[5]

Abstract

Analysis of seafloor backscatter collected from single and multi beam echosounders (SBES and MBES) has been carried out using a theoretical model and experimental data. The aim of this work was to evaluate backscatter parameters for the purposes of seafloor habitat classification. A theoretical model developed by CMST was used to study the backscatter properties depending on seafloor properties, depth and transmit pulse width. Peak intensity and energy calculated from the predicted mean envelop for different sediment types were shown to be proportional to the backscatter coefficient. Integration of the tail of the envelope, which results in a commonly used backscatter parameter E1, shows that accurate calculation of the insonfication area is required to make it independent of depth. The effective pulse width of seafloor echoes was found to be proportional to the backscatter coefficient and highly dependent on the transmit pulse width and depth. Experimental measurements using a Simrad EQ60 single beam echo-sounder, operating at 38 and 200 kHz, were made to distinguish different seafloor habitats. The energy and parameter E1 at 200 kHz were the most useful parameters for discriminating different seafloor habitats and the resulting classification was consistent between different transects across the same area of the seafloor. In addition, temporal variations of backscatter from seagrass were studied. This experiment showed unexpectedly small temporal variations in the mean backscatter characteristics, both intensity and energy, at 200 kHz. Subtle diurnal variations were observed in the mean backscatter intensity at 38 kHz. Statistics of backscatter from seagrass was analysed at both frequencies pointing out a complex, rather bimodal distribution observed in the fluctuations of the instantaneous backscatter intensity.

Author: Maria Desamparados Torres Medina, email: mariam.tmedina@gmail.com

Date of issue: July 2010

INDEX

A tot i tots el que han fet possible que esta experiencia fora real, sobretot per als que estaven prop de mi.

Gràcies.

I. INTRODUCTION

1. MOTIVATION

One of the key challenges in the study of the natural environment is determining what change is due to natural variability and what can potentially be a result of anthropogenic impact to the system. Coastal habitats, such as seagrass and coral reefs, are significant forces that shape our ecosystem and are intrinsically linked with the overall health of the environment [1]. Coastline change has been recognized as a likely future challenge to coastal management, due to the increased coastal utilization. Measuring impacts from industrial contamination, urban growth and general nutrient enrichment on coastal habitats, e.g. significant seagrass loss to the ecosystem, is not a trivial exercise. Therefore, methods that can accurately measure change in the marine environment are required for effective management of natural resources.

One such important coastal habitat is seagrass, as it: 1) plays a critical role in maintaining marine biological productivity and biogeochemical cycles, e.g. through photosynthesis they produce large quantities of oxygen [2]; 2) supports a high species diversity and commercial fisheries [3]; 3) creates natural barriers, and thus strongly reduce coastal erosion; and 4) is an important indicator of disturbance in the coastal marine environment. Hence, there is a scientific interest in and practical importance of estimating the extent of existing stocks and measuring changes over time. However, monitoring marine habitats, such as seagrass, is both economically and technically challenging. Detection and measurements of submerged aquatic vegetation has been carried out using several methods. These different methods can be grouped into two large types: direct sampling and remote sensing techniques [5][7][8][9][10][11].

Many studies have a requirement for assessments of seabed type: defence related (e.g. mine countermeasures), environmental (e.g. habitat mapping and protection), economic (e.g. fisheries, mining), and maritime (e.g. dredging of harbours and channels). Remote sensing combined with direct sampling methods (ground-truthing) is the most common approach to seafloor habitat mapping. Acoustic remote sensing of the seafloor has been used to discriminate between different seafloor habitats, particularly in deep or turbid waters where aerial remote sensing is not effective.

Acoustic remote sensing of the seafloor is usually carried out using a sonar (*SOund, NAvigation and Ranging*) system, which is an instrument used for getting information about the underwater environment through the transmission of sound waves and measuring the return echoes. Sonar mapping systems are usually deployed from vessels and are operated while underway. Some of sonar systems

can be used to determine the bottom type. Acoustic data usually require ground-truthing to help assign seafloor types to any classification map produced. The results can also be dependent on echosounder characteristics, such as frequency and beamwidth (discussed in the next chapter). One such sonar mapping system is a Single Beam Echosounder (SBES). This type of echosounders is simple to use and is found on most vessels. The primary purpose of the SBES is to measure the two-way travel time of the signal, which gives the local water depth. In addition, the shape and amplitude of the echo received can be used to derive information about the type of seabed. It is the use of the SBES in seafloor classification that is the subject of this project. This study has analysed the energy and the envelope of the received backscatter signal from SBES experimental data and model predictions, with the purpose of improving the classification of seafloor habitats. Some data from a multibeam sonar system have also been analysed.

2. AIMS AND SCOPE OF THE STUDY

There were two main aims of this study:

1. Evaluate different parameters derived from the backscatter envelope measured using a SBES to determine the most useful backscatter characteristics for seafloor habitat classification.
2. Measure the temporal variability of backscatter characteristics of seagrass.

Following the introduction, this dissertation is divided into the following chapters:

- Chapter 2: Background Theory. This presents a background to understanding the physics of seabed backscatter, which is essential for the classification methods, as well as an explanation of how SBES systems work and the signal backscattered from the seafloor is processed.

- Chapter 3: Modelling seafloor backscatter envelopes from single beam echosounders. A theoretical model was use to predict the shape of backscatter envelope received by SBES from different kinds of sediment. The model was developed by the Centre for Marine Science and Technology (CMST),at Curtin University of Technology in Perth, Australia. The CMST model uses the Applied Physics Laboratory (*APL*) high-frequency bottom scattering model [34][35] to determine the backscatter coefficient based on the sediment characteristics. Parameters derived from the backscatter envelope, such as peak intensity and energy, were analysed with respect to their dependence on the seafloor backscatter coefficient, sea depth and transmit pulse width to determine their effectiveness in discriminating different seafloor types.

- Chapter 4: Analysis of single beam echosounder backscatter data collected from different seafloor habitats. Data collected with a SBES over a sand-seagrass transition and over a coral reef-sand-seagrass transition have been processed and analysed. The main focus of this chapter is the correlation of backscatter parameters with changes in seafloor habitat type.

- Chapter 5: Temporal variability of backscatter collected over seagrass. In the last part of the dissertation, the objective was to determine whether there is time dependence in backscatter collected over vegetated seafloors. Gas bubbles released from seagrass due to photosynthesis and/or respiration are one of the most likely sources of strong acoustic scattering. If this is so, then the backscatter level from seagrass could vary with time, as the rate of gas emission could change during the day and in different seasons due to changes in the sun illumination. Using a Simrad EQ60 single beam sonar, backscatter from bare sediment area (sand) and from dense seagrass (*Posidonea*) was measured at 38 and 200 kHz every 2 s over 2 and 7 days respectively.

- Chapter 6: Conclusions. The dissertation ends with a comparison of the study's findings with results of other studies. Also, recommendations for further work in the field of acoustic seafloor classification are made.

II. BACKGROUND THEORY

1. PHYSICS OF SOUND AND SCATTERING

INTRODUCTION

Waves of sound energy oscillates back and forth in the direction the wave is travelling. They comprise of alternative compressions and rarefactions that propagate at a speed that depends on the characteristics of the medium, such as bulk density, compressional wave speed and attenuation [15]. Conceptually, a sound wave travelling diminishes in intensity over distance due to transmission loss caused by spreading and absorption. The spherical spreading loss [42] is the major component which causes this effect, implying that the intensity or the mean square pressure varies inversely with the square of the distance from the source (e.g. sound levels diminishes 6dB when the distance is doubled). In addition, when the sound wave interactions with the seafloor, "reflection" and "scattering" occur. Reflection of a sound wave at a surface diffuses the wave out (with some energy loss) in a returned wave with an equal angle to the angle of the incident wave ("specular direction"). Scattering produces a distribution of acoustic energy over angles other that the incoming wave. The scattering returned to the source (e.g. as in an echosounder) is referred to as backscatter. This chapter discusses what influences backscatter, how it is measured using a single beam echosounder and how these backscatter measurements can be used to identify seafloor habitats.

REFLECTION AND SCATTERING

Scattering from the seafloor is usually quantified in terms of "scattering coefficient" [44], in which an insonification area is situated in the far field[1] of the source, as shown in Fig. 3.

$$\sigma_{bs} = \frac{I_s R_1^2 R_2^2}{I_i R_{\mathrm{Re}\,f}^2 A} \tag{1}$$

where: I_i is source intensity at a reference distance R_{ref} (usually 1m), $I_s = \langle p_s p_s^* \rangle / \rho c$ is the mean intensity of the scattered signal at the receiver (p_s is the acoustic pressure in the received signal), R_1 is the range from the source to the seafloor, R_2 is the range from the seafloor to the receiver, and A is the

[1] The 'far field' is where the range of the differential distances to the elements is greater than the 'critical range' and there are no peaks and troughs of interference

area of the scattering surface (<…> means statistical averaging). In this study, the scattering coefficient is measured in a monostatic arrangement, and thus R_1=R_2. Loss of energy through absorption in the water column must be taken into consideration at high frequencies. The absorption loss is usually defined as βR (dB), where β is the absorption coefficient (dB/m). Consequently, for this study the surface scattering coefficient is calculated as:

$$\sigma_{bs} = \frac{I_s R^4 \exp(2\alpha R)}{A I_i}, \quad \alpha = \beta / 20\log(e). \tag{2}$$

The surface scattering coefficient is a dimensionless quantity that accounts for the intensity (power) ratio of the incident and scattered waves determined per unit area at a reference distance of 1m. When expressed in dB, it is commonly called the backscatter strength (BS):

$$BS = 10\log_{10}(\sigma_{bs}) \tag{3}$$

The level of backscatter strength measured from the seafloor is influenced by various properties, such as the impedance contrast between the water column and seafloor, surface roughness and volume heterogeneity (Fig. 1). For instance, high-porosity sediments, such as silts and clays have a low acoustic impedance contrast with the overlying water so reflect and scatter considerably less energy compared with high-density material like gravel and rock, which have a much higher impedance contrast.

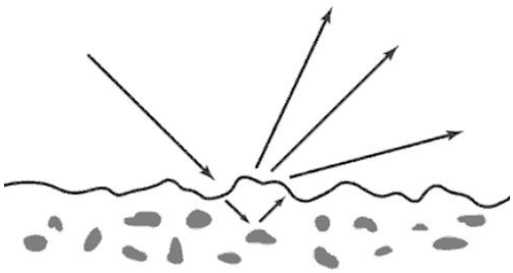

Fig. 1. Sketch showing acoustic scattering due to the roughness of the water sediment interface and heterogeneity of the sediment. Image extracted from ref. 35.

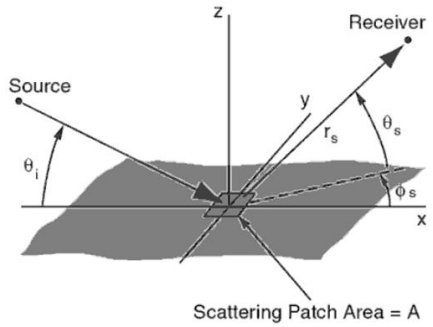

Fig. 2. Definition of angular coordinates used in treating reflection and scattering. Image extracted from ref. 35.

If the seafloor is rough and/or heterogeneous on scales comparable to the acoustic wavelength, it will scatter sound energy over a distribution of directions. So, the amount of scattering of acoustic energy is a factor of the seafloor roughness and acoustic frequency. For instance, surfaces which appear rough to short acoustic wavelengths will appear smooth to long acoustic wavelengths. In addition, the angle of incidence can strongly influence the backscatter level. At angles of incidence near vertical, backscatter is dominated by specular reflection and large scale roughness; whereas, at moderate and large incidence angles backscatter is made up of contributions of small scale roughness and volume heterogeneity. As a result, over a homogenous seafloor, backscatter strength usually decreases as the angle of incidence increase. The relationship between backscatter strength and incidence angles is dependent on seafloor properties, thus has been used for seafloor classification [7].

BUBBLES

A constant and almost unpredictable heterogeneity which causes significative changes in the scattering strength of the signal are bubbles. The amount and size distribution of bubbles is sensitive to physical, chemical and biological processes which are very specific to each environment such it is the photosynthesis of vegetated habitats. It is known that gas bubbles in seawater have a profound influence on sound propagation because their high acoustic impedance compared to the water. Moreover, the presence of bubbles of many sizes, cause scatters attenuation and dispersion in a way that depends on the resonance frequency of the bubbles [44]. In this dissertation, because of the continuously measurements over the time in vegetated area in the experimental part, bubbles are an interesting environmental factor and also they are in general the underwater acoustic field.

2. SINGLE BEAM ECHOSOUNDERS

A SOund NAvigation and Ranging (SONAR) system is an instrument used for getting information about the underwater environment through the transmission and receiving of sound waves. One common method to carry this out this is through electro-acoustic transducers, such as in single-beam echosounders (SBES). In this dissertation, a SBES has been used to acquire backscatter information from the seafloor. Although more sophisticated sonar systems (e.g. multi-beam sonar or sidescan sonar systems) are available, they can be both cost and technically prohibited. Whereas, SBES are simple to use and widespread on nearly all vessels.

A SBES system transmits vertically bellow the ship a short signal in a beam of average angular aperture (Fig. 4). The system measures the two-way travel time of the signal, which gives the local water depth and can provide information about the kind of seabed or detecting fish, depending on the selected frequency. The first return from the seabed corresponds to points closest to the ship, and further as the cone spreads contributions from sub-surface penetration and, if present, overlying biota such as seagrass.

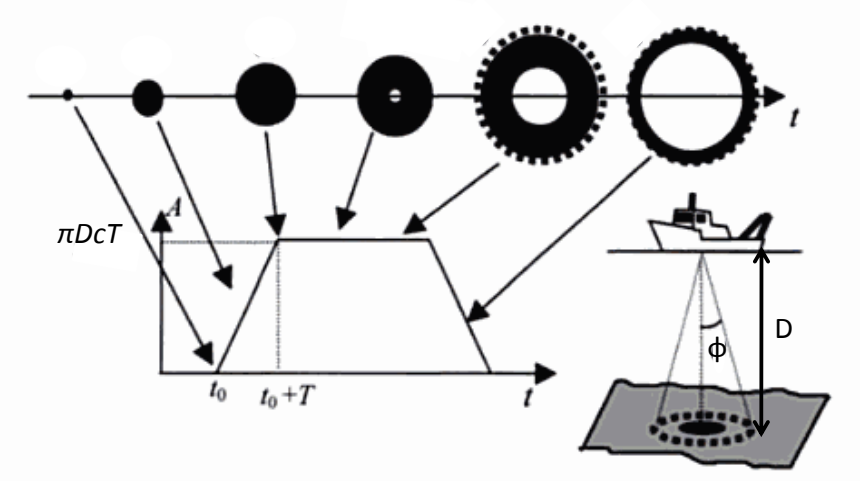

$$A = \pi (D \tan (\Phi))^2 \quad (4)$$

Fig. 3. Schematic representation of the insonification of the seafloor from a SBES.

Where: D equal to depth and Φ equals to half-power beam width. It is important to know the characteristics of the produced insonified area. The area insonified on the seafloor by a SBES (A) is dependent on the beam width, water depth and the local slope (Eq. .

Because of wavefront curvature a ping from an echo-sounder with a wide angle beam ensonifies first a circle on the seabed, then progressively ensonifies an annuli of increasing radii and higher incidence angles (Fig. 3.).

OPERATION

Over this dissertation, all the data collected from a single-beam echo sounder (*SBES*) has been obtained using the *Simrad EQ60* echo sounder, designed for the professional fishery community. The frequencies studied have been 38 kHz and 200 kHz and the pulse length has been adapted to the medium characteristics (appendixes) for each case. This *Simrad EQ60* system, like many SBES, was not calibrated, but backscatter values can be used on a relative scale. Horizontal resolution (distance between two successive sampling points on the sea bottom), depends basically on the data acquisition throughput and the speed of the vehicle carrying the sonar: the highest is the number of acquired samples, the longest is the time spent to acquire the scanline data and the worst the resolution on the bottom. In the case of a poor horizontal resolution, columns in the resulting sonar images are poorly related to their adjacent ones. Whereas, vertical resolution depends on the transmitted pulse duration and the number of acquired bings. For example, a pulse length of 1.024ms gives a vertical resolution of 19.2cm, whereas a pulse length of 0.256ms gives a vertical resolution of 4.8cm. If the vertical distance between echoes is less than this, the two echoes will be shown as one. So, the vertical resolution of the echogram increases with a shorter length. Hence, a balance must be found between the desired vertical resolution and the speed of the carrier.

Fig. 4. Photo of the SIMRAD EQ60 into the seawater during the experimental part.

ACOUSTIC SEAFLOOR CLASSIFICATION

The backscatter envelope recorded by SBESs represents the variation of amplitude with time, which also relates to the angle of incidence. Hence, there are a variety of parameters derived from backscatter envelope recorded by SBES that have found to be useful in seafloor classification [e.g. 5, 8, 12, 28]. Commonly used parameters include the backscatter strength based on the energy and intensity of the seafloor envelope [28], which are referred to in this study as the surface scatting coefficient based on energy (SSCE) and the surface scatting coefficient based on intensity (SSCI). Also, the energy of the tail of the seafloor envelope (Fig. 5), referred to as E1 [ref - Chivers et al 1990], has been found by many authors to be a very useful in discriminating different seafloor habitats as it ignores the contributions from specular refection. More recently, [8] found the effective pulse width (EPW) was useful for identifying areas of vegetated seafloor, such as seagrass.

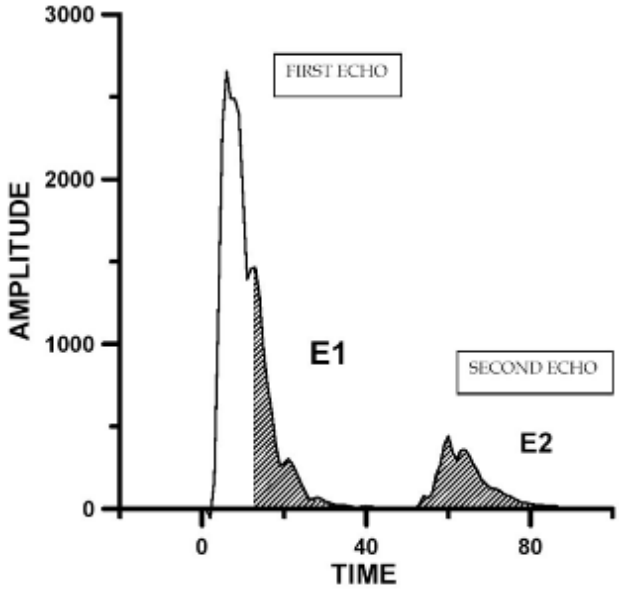

Fig. 5. The parts of the first and second bottom returns. Energy of the shaded regions is integrated to form two indices - *E1* (for the tail of the first echo – summation begins one pulse length from the echo start) and *E2* (for all the second echo). From Hamilton (2001).

In this study, the different seafloor parameters are evaluated for their ability to discriminate different seafloor habitats. The first part of the investigation is to use a SBES model to investigate the relationship between these SBES parameters and depth, transmitted pulse width and the backscatter coefficient of the seafloor (Chapter 3). Then SBES data collected from different seafloor habitats area analysed to determine their ability to discriminate different seafloor habitats (Chapter 4). In Chapter 4

uses comparison with towed video data, the Fisher Criterion, and Probability Distribution Function (PDF) to help evaluate the different SBES parameters.

Underwater video analysis of coincident sections of the same SBES transect (using the head, latitude, longitude), connected simultaneously to a GPS unit was carried out. The classification of the habitats from the video is done by eye, visualizing and noting the seafloor sediment type along the transect for each frame number to correlate to a position.

The *Fisher Criterion is* the *distance* between the means of the two classes normalised for the variance within each class:

$$J(w) = \frac{\left|m_1 - m_2\right|^2}{s_1^2 + s_2^2} \tag{5}$$

where m represents the mean, s^2 represents the variance, and the subscripts denote the two classes. The higher the Fisher Criterion the more separated the classes, the value has to be greater than 1 for any class separation.

PDFs are a function that describes the relative likelihood for this random variable to occur at a given point in the observation space. The probability of a random variable falling within a given set is given by the integral of its density over the set. It is also useful to plot the probability of false alarm (1-CDF) in a logarithmic scale to see the trend in the tail. PFA plots are used in Chapters 4 and 5 for understanding the underlying scattering processes. For instance, Gaussian scattering will result in the variation of SSCE to be well modelled by a Gamma distribution.

III. MODELING SINGLE BEAM ECHO SOUNDER BACKSCATTER

1. INTRODUCTION

The aim of this chapter is to use a theoretical model developed by the *CMST* to predict the backscatter envelope received by single beam echo sounders (Gavrilov, 2008) from different kinds of sediments, in order to evaluate different parameters [45] used for seafloor classification. The single beam backscatter characteristics studied in this dissertation were:

- Surface Scattering Coefficient derived from the backscatter Energy (*SSCE*).
- Surface Scattering Coefficient derived from the backscatter Intensity (*SSCI*).
- Backscatter energy in the tail of the echo signal (*E1*) [17] and Effective Pulse Width (*EPW*) of backscatter envelope, which have been found to be important for seafloor classification in other related studies [8].

These characteristics were calculated for the backscatter envelope predicted numerically from the CMST model for different seafloor types. The surface scattering coefficient (or seafloor backscatter strength) derived from these backscatter characteristics was then compared to the values used as input parameters in the envelope model to evaluate the ability of measured backscatter characteristics to discriminate different seafloor types. Previous studies have found that certain single beam parameters can be dependent on depth and pulse width, e.g. E1 (Kloser et al, 2001). So, parameters calculated from the envelope, were also tested to see if there was any dependence on sea depth or pulse width.

2. MODEL DESCRIPTION

The model used in this study is part of a suit of algorithms developed by *CMST* for the purpose of investigating interference between different sonar systems deployed from the same platform and operated at the same time (Gavrilov, 2008). A detailed description of the *CMST* model is given in Gavrilov (2008), below is a summary.

The algorithm developed by *CMST* uses the *Applied Physics Laboratory* (*APL*) model [34] to predict the seafloor backscatter coefficient based on seafloor properties. Ten types of sediments were modelled; rough rock, rock, gravel, very coarse sand, coarse sand, medium sand, fine sand, very fine sand, silt and clay. Very fine sediments composed mostly of clay are often *"slow",* which means that sound is refracted downward toward the vertical. Sound incident on a *"fast"* sediment is refracted toward the horizontal and tends to penetrate to a lesser depth. The backscattering model is very sensitive to the spatial spectrum of the surface roughness for coarser sediments and becomes less

sensitive for finer sediments. Parameters linked to the sediment roughness are interpolated in the *APL* method, and there exists a strong correlation between the sediment type and its roughness characteristics. The bottom backscattering strength (Eq.6) is a sum of surface and volume components and is a function of the bottom parameters: density, sound speed, sound attenuation, spectral exponent and spectral strength of the surface roughness, volume inhomogeneity spectrum and some others. It is also dependent on acoustic frequency and grazing angle.

$$S_b = 10 \cdot \log_{10}(\sigma_{surface} + \sigma_{volume}) \tag{6}$$

There is strong correlation between the energy and intensity of backscatter and the backscatter coefficient $\sigma = \sigma_{surface} + \sigma_{volume}$ (Fig. 7). The surface roughness component ($\sigma_{surface}$) of the backscatter coefficient is evaluated as an input parameter for the envelope model. The volume scattering component (σ_{volume}) was set to zero to simplify calculations because its contribution at vertical incidence of SBES is much smaller than that of the surface component (Gavrilov, 2008).

The model characteristics were chosen similar to those used in the experimental work, e.g. *Simrad EQ60* sonar parameters and settings and environmental characteristics. The input parameters used in the algorithm are explained below:

- Frequency of the transducer, which was 200 kHz in this study. Although measurements with the 38 kHz transducer were also taken, the 200-kHz backscatter data appeared to be much more useful for the purposes of seafloor classification [8].
- Pulse length: *Simrad EQ60* transmits signal between 100 and 1024μs long. Several values were tested.
- Sediment properties, such as mean grain size, porosity, ratio between sediment and water density, velocity and absorption and surface roughness spectrum [34]. Physical characteristics of the water column, such as the sound speed in water and sea depth.
- Measurement conditions, such as the location of the transducer (depth), sampling frequency.
- Range to the bottom: varying from 5 m to 50 m. Depth dependence analysis is needed to examine how envelopes evolve with increasing range.

Evaluation of the seafloor scattering coefficient involves numerous equations, beginning with the roughness scattering component modelled with three different approximations (Kirchhoff, Composite Roughness and Large-Roughness Scattering approximations applied in different angular domains[34]), and ending with the sediment volume scattering coefficient. The resulting seafloor scattering

coefficient is found as a function of incidence angle by interpolating results obtained in different angular domains.

3. CORRELATION OF SINGLE BEAM BACKSCATTER CHARACTERISTICS WITH THE SEAFLOOR BACKSCATTER COEFFICIENT

There are several parameters that can be derived from single beam backscatter envelopes, but to be useful in seafloor classification they need to be able to distinguish different seafloor types. Fig. 6 shows envelopes modelled for the different seabed types using the *CMST* model. The *'harder'* and *'rougher'* beds, such as rock and gravel, have higher peak intensities in the envelope than *'softer'* and *'smoother'* ones, such as clay. Hence, there is an evident correlation between the backscatter coefficient and the peak intensity (Fig. 7a) and energy (Fig. 7b) of the envelope. *EPW* also shows a strong correlation though it has been shown not to be sufficiently robust for seafloor classification due to its strong dependence on range to the bottom. The *E1* parameter (Fig. 7c) has the strongest correlation with the seafloor backscatter coefficient among all the variables studied. Therefore, the *E1* parameter is likely to be one of the most useful parameters in seafloor classification.

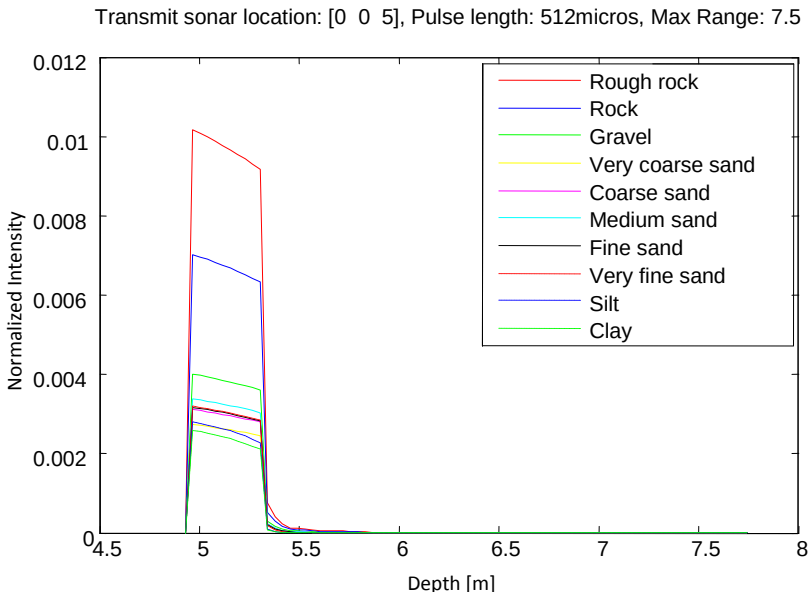

Fig. 6. Example of backscatter strength envelopes modelled numerically using the CMST model for the different sediment types for 5 m water depth and 512μs pulse length.

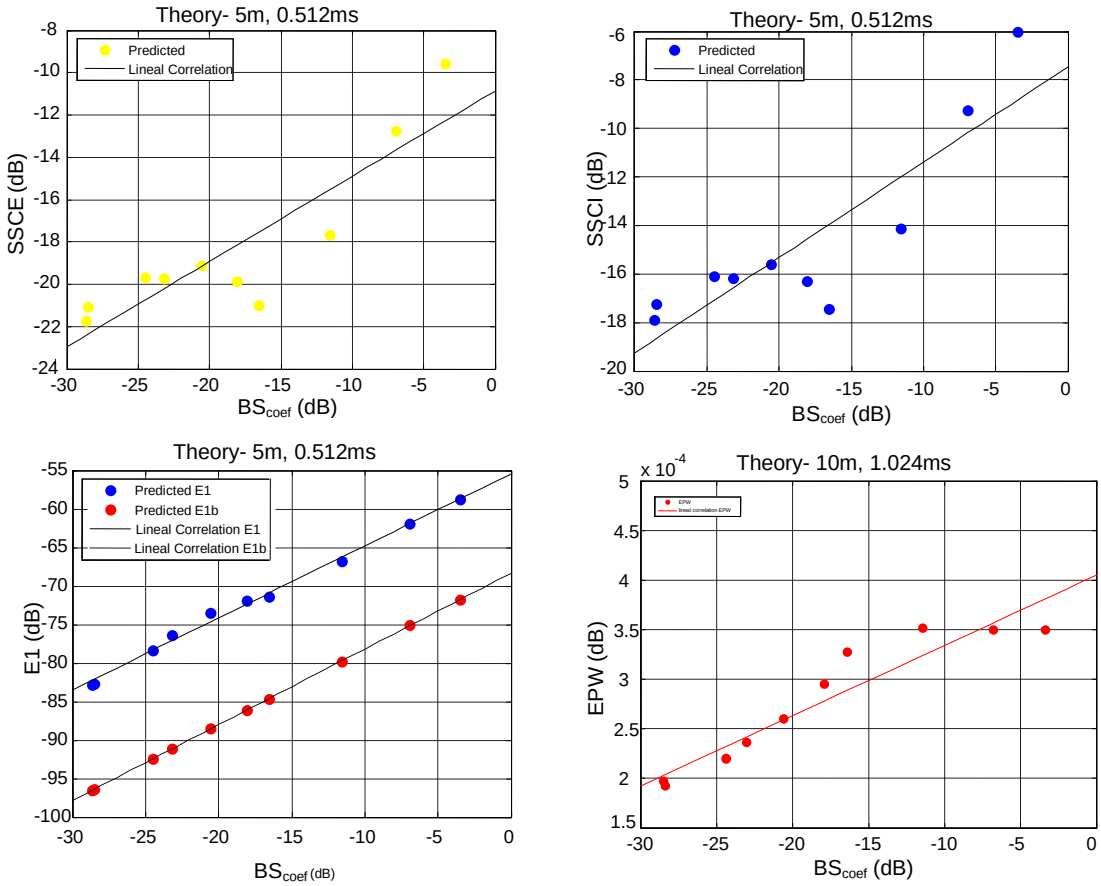

Fig. 7. Different characteristics of backscatter echoes as a function of the seafloor backscatter strength (dB) approximated with linear regressions. Sea depth is 5m, pulse width is 256μs. The characteristics of backscatter echoes are: backscatter energy (SSCE) (top left panel), backscatter intensity (SSCI) (top right panel), E1 (bottom left panel), and Effective Pulse Width (EPW) (bottom right panel).

4. DEPENDENCE OF SINGLE BEAM BACKSCATTER CHARACTERISTICS ON DEPTH

Even if the bottom sediment type remains the same, the shape of the backscatter envelope and the power of the returned signal can change significantly with depth. So, it is necessary to know the influence of sea depth on the estimates of the seafloor backscatter strength derived from the backscatter signal energy and intensity.

Fig. 8 shows estimates of the seafloor backscatter coefficient (SSCE) of different seafloor types derived from the backscatter energy at different ranges from the sonar head to the bottom. There is no range dependence observed in the *SSCE* estimates (Fig. 8a). The same behaviour was observed for the

seafloor backscatter coefficient estimates from the backscatter intensity (*SSCI*). However, the range dependence is significant for E1 (Fig. 8b) and so it is for the EPW. This means that changes in the sea will affect estimates of the seafloor backscatter coefficient and, hence, results of acoustic classification of the seafloor.

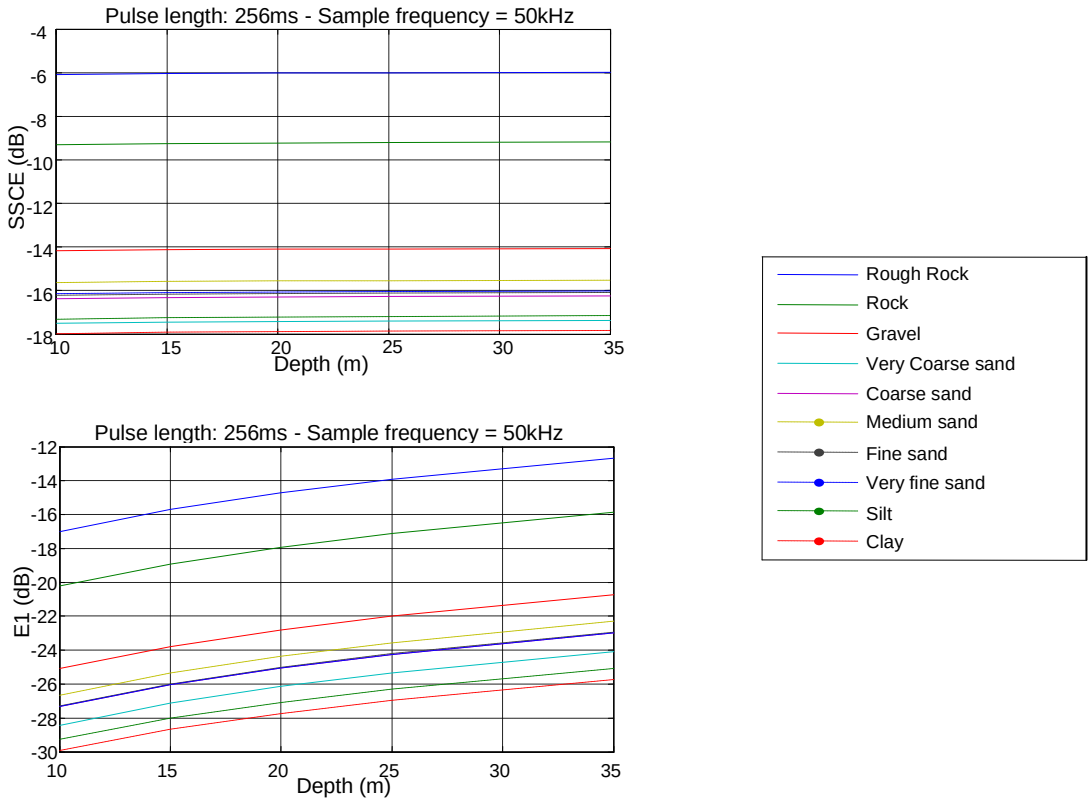

Fig. 8. a) *SSCE* estimates for different sediments made for a transmitted pulse of 256 μs long for different sea depth from 10 to 35 m b) Estimates of parameter E1 made for the same pusle length, ranges to the bottom and sediments.

Although *E1* was found to be most correlated with the seafloor backscatter strength at a fixed range to the bottom, it is not the best parameter for seafloor classification because of its significant dependence on sea depth. For instance, the value of *E1* for clay at a certain depth is similar to that of sand at a shallower depth (Fig. 8b). Therefore, the E1 parameter needs to be properly corrected for sea depth before it is used for seafloor classification. The cause of the depth dependence in E1 was found to be an inadequate correction for insonification area. In the original algorithm [45], *E1* is normalised by the

footprint area. However, the backscatter envelope in the echo tail is not correlated to the footprint area, but for the instantaneous insonification area. The new algorithm for integration of the echo tail, which makes correction for the insonification area rather than the footprint area, results in a different parameter called $E1_b$ to distinguish it from the original *E1*parameter. This new parameter $E1_b$ corrected properly for insonification area is no longer dependent on sea depth (Fig. 9).

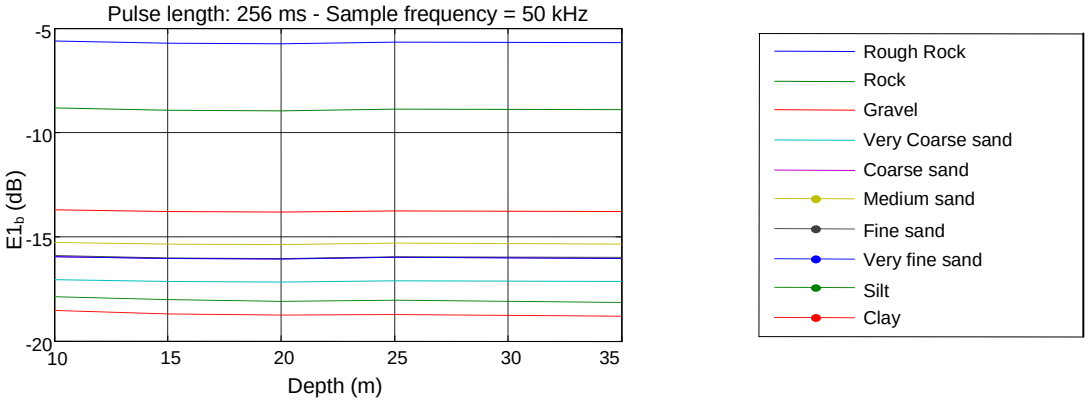

Fig. 9. Energy of the bottom echo tail corrected the insonification area (***E1*$_b$)** calculated for a transmitted pulse of 256 μs long at different sea depth from 10 to 35m for different sediments.

5. DEPENDENCE OF SINGLE BEAM BACKSCATTER CHARACTERISTICS ON PULSE WIDTH

If sea depth is not changing but the transmitted pulse length, the seafloor backscatter coefficient derived from the energy and intensity of backscattered signals shows rather negligible dependence on the pulse length. This was expected as the backscatter energy is normalised for pulse length, and the peak intensity is normalized by the insonification area, which takes into account the range from the sonar head to the seafloor. The *E1*parameter was found to have some dependence on pulse length. However, the $E1_b$ parameter, which is corrected for insonification area, shows negligibly small variations with pulse length (Fig. 10).

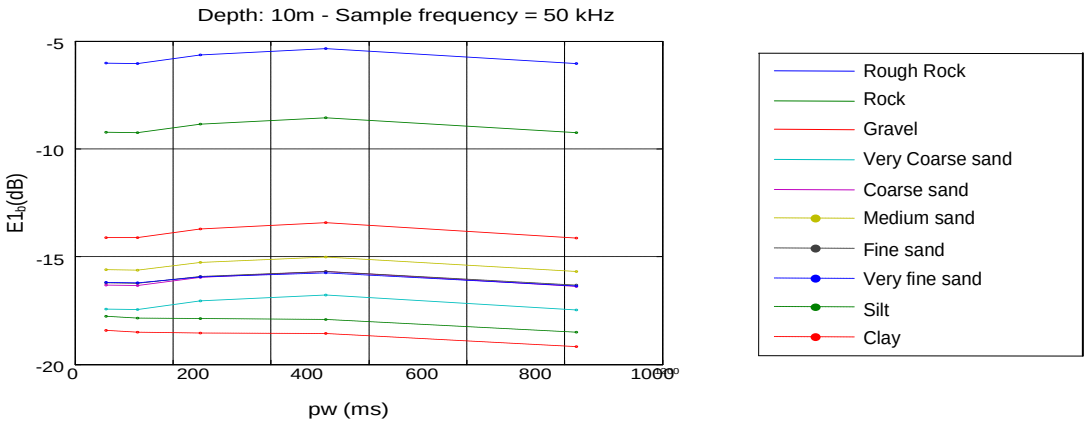

Fig. 10. Energy of the bottom echo tail from different sediments corrected the insonification area ($E1_b$) calculated for a sea depth of 10 m and transmitted pulse length varying from 64 to 1024 μs.

6. DISCUSSION

The dependence of estimates of the seafloor backscatter strength, derived from different characteristics of the backscatter envelope measured by SBES, on sea depth and transmitted pulse length was examined in order to determine the most robust SBES backscatter characteristics to be use for seafloor classification. Some dependence on sea depth and pulse length was found for the *E1* parameter, but a modification of it, the $E1_b$ parameter corrected for the insonification area, appeared to be much less dependent on sea depth, which makes it appropriate for seafloor classification over areas of varying bathymetry.

IV. MEASURING SINGLE BEAM BACKSCATTER CHARACTERISTICS FROM DIFFERENT HABITATS

1. INTRODUCTION

SBES has shown to be a useful tool in seafloor habitat mapping (Sotheran, Foster-Smith and Davies, 1997). A variety of different parameters derived from SBES backscatter data have been shown to be useful in distinguishing different seafloor types (bare sediment, seagrass, coral reef, muddy beds, etc.). These parameters are the backscatter energy and instantaneous intensity, the effective pulse with and the E1 parameter, characterising the seabed roughness (See Chapter 2 for more detail of these parameters) .

The aim of this Chapter is to evaluate the ability of these different SBES parameters to discriminate different seafloor habitats. This study was carried out using data collected with a SBES along two different transects that crossed different seafloor habitats including seagrass, coral reef and sand. The SBES data were processed using an algorithm developed by the Centre for Marine Science and Technology (Parnum, 2009), which calculates the different backscatter parameters discussed above. The Fisher criterion was used to assess the ability of the different SBES parameters to discriminate different seafloor types. In addition, a statistical analysis of backscatter fluctuations was carried out to further understand the backscatter processes from different seafloor habitats and, in particular, to examine if the backscatter process is Gaussian. Details of the seafloor acoustic scattering theory and backscatter statistics can be found in Chapter 2 (background). The SBES data processing techniques adopted in this study provide an alternative to the commercially available bottom classifiers.

2. METHODS

DATA COLLECTION

A Simrad EQ60 single beam echosounder (SBES), operating at 38 and 200 kHz, was used to collect seafloor backscatter from two different areas of Australia:

1. Owen Anchorage in Western Australia.
2. Morinda Shoal in Queensland, Australia .

SBES data were collected on 21st October 2005 in Owen Anchorage, which is a shallow water area (<20 m) within Cockburn Sound, Perth, Western Australia. From the previous ground-truth information, seagrass (*Posidonia*) was known to be present in the shallow eastern side of the transect;

whereas, an unvegetated seabed composed mainly of sand and muddy sand was present in the deeper western side of the transect [26].The transmit pulse duration used at 38 kHz and 200 kHz was 4096μs and 1024μs respectively.

The reef-capped Morinda Shoal is located north-east of Cape Bowling Green (Queensland) and is situated in the central section of the Great Barrier Reef Marine Park. Three parallel transects collected SBES data over Morinda Shoal on 20th August 2004. During one of the transects, a towed underwater video was deployed. The video survey found a hard standing *coral* reef and *coral* rubble, tropical *seagrass* and bare sediment present. Fig. 11 shows an example of a captured frame of the towed underwater video.

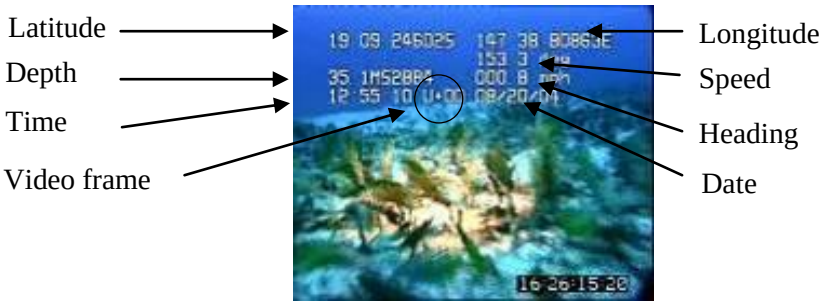

Fig. 11. Captured frame of Morinda Shoal video. All the parameters showed in the frame give the location of video recordings and the video settings.

DATA PROCESSING

The SBES backscatter data was used to analyse the backscatter intensity at the bottom detection point (*SSCI*), the energy from the whole of the first echo (SSCE), the energy from just the tail of the first echo (*E1*), the energy from the whole of the second echo (*E2*), and the effective pulse width (*EPW*) of the first bottom echo. The Centre for Marine Science and Technology (CMST) developed a set of algorithms in *MATLAB* to read and process data obtained from the *SBES Simrad EQ60* (Parnum, 2009). This processing was broken down into 2 main steps, which are:

- *Convert Simrad binary fileswith raw data to Matlab files*: backscatter power data were converted to surface and volume backscatter characteristics and GPS coordinates were interpolated to georeference backscatter characteristics measured by each sonar ping. Files were broken up into sections of 500 pings,

- *Main processing:* The sections for each original file were recombined and processed to calculate for each ping:
  i. Depth (m), and
  ii. Seafloor backscatter parameters (including *E1* and *E2*)

More details on the seafloor backscatter parameters and the MATLAB SBES toolbox can be found in the introduction and in Parnum (2009) respectively.

DATA ANALYSIS

The seafloor backscatter characteristics derived from the SBES data were grided into 100 m cells to analyse along track changes. Probability density functions (PDFs) of variations in backscatter characteristics and a Fisher criterion for distinguishing different distributions for different seafloor habitats were calculated to assess the ability of the different characteristics to discriminate different seafloor types. The Probability of False Alarm (PFA) was calculated for normalised values of backscatter energy to assess whether the scattering processes from the different seafloor habitats could be modelled by a number of selected model distributions, including those for a Gaussian process.

3. RESULTS

OWEN ANCHORAGE - SBES DEPTH AND BACKSCATTER PARAMETERS

Fig. 12 shows the sea depth along the two parallel transects across the Owen Anchorage survey area. The backscatter characteristics *E1, SSCE, SSCI* and *EPW* measured at 200 kHz along these transects are shown in Fig. 13. At 38 kHz, there was a little difference between the distributions of the backscatter parameters measured from different habitats. However, the difference in the distributions at 200 kHz is noticeable and, therefore, the backscatter characteristics at 200 kHz were used for seafloor classification. The discrimination of two different habitats with the *E1* parameter at 200 kHz is quite good, as shown in Fig. 14. The *SSCE* parameter also provides reasonable discrimination. Apparently, *SSCI* appeared not to be a good parameter for this purpose, neither the *EPW*, as also seen in Fig.14

Table 1 gives the *Fisher criterion* for the different SBES parameters at 200 kHz. The *SSCE* and *E1* parameters at 200 kHz both have values greater than unity.

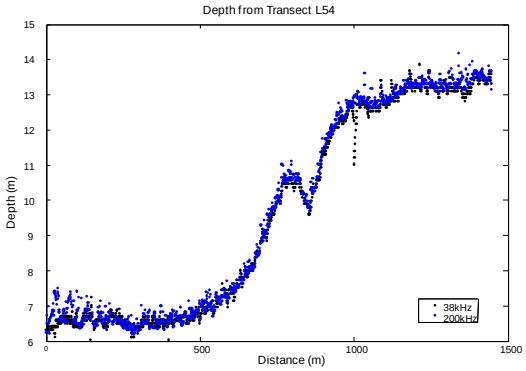

Fig. 12. Depth calculated from the sonar data at 38 kHz and 200 kHz.

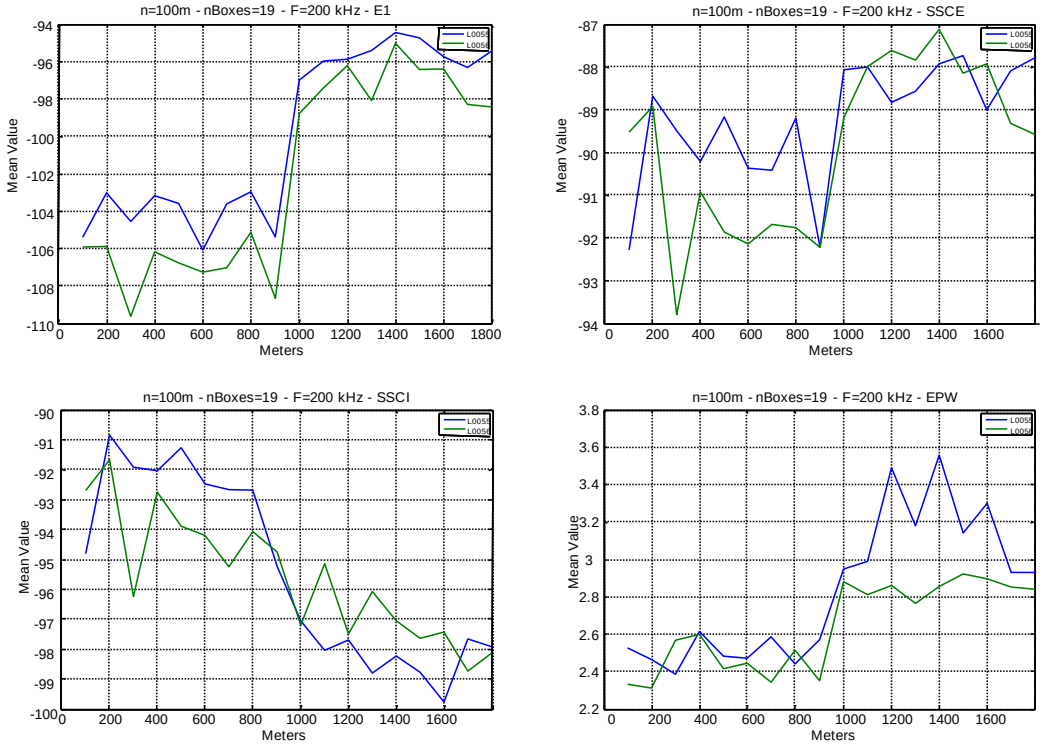

Fig. 13. Backscatter characteristics at 200 kHz averaged over 100-m sections of transects: *E1* (top left), *SSCE* (top right), *SSCI* (bottom left) and *EPW* (bottom right)

Fisher Criterion	E1		SSCE		SSCI	
Transect	**L055**	**L056**	**L055**	**L056**	**L055**	**L056**
Linear Data	1.824233	1.615829	0.167947	0.282942	0.747347	0.245258

Table 1. Fisher criterion for each interested backscatter parameter.

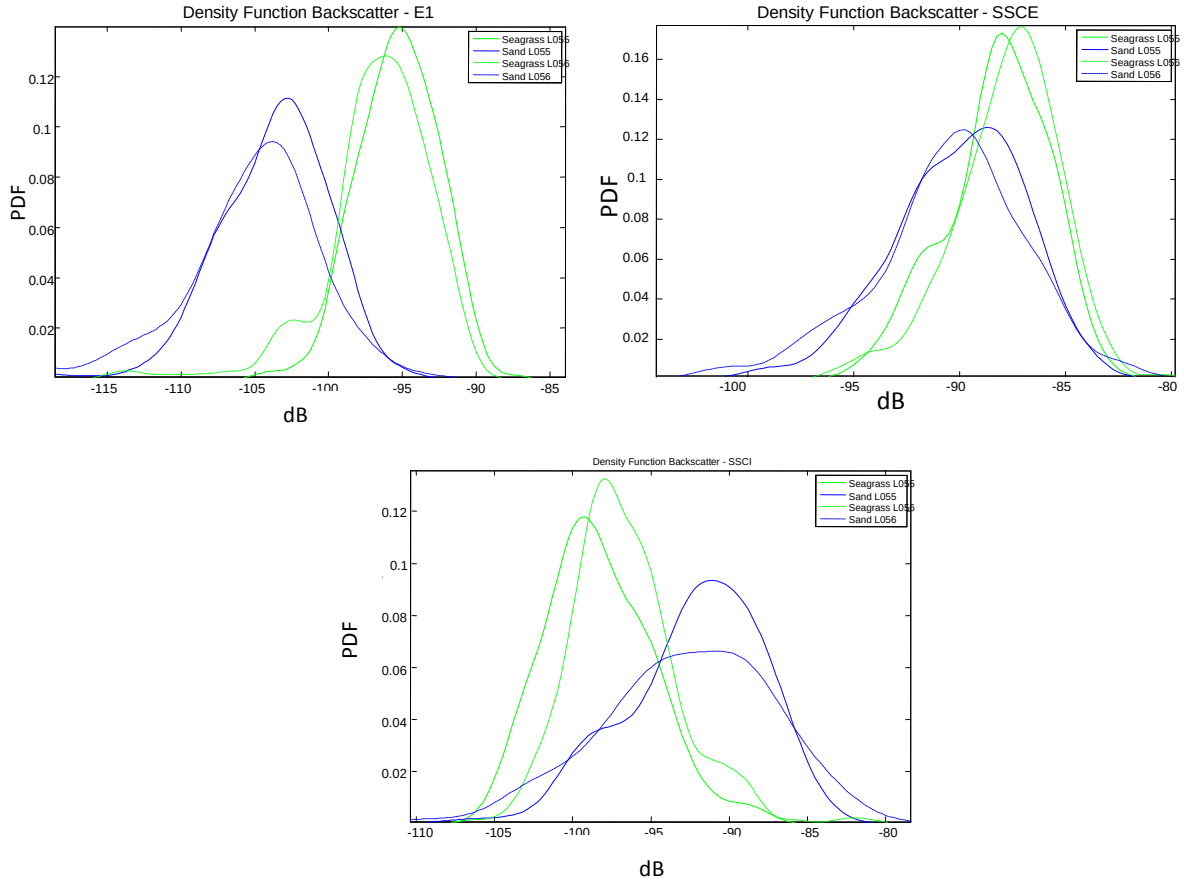

Fig. 14. Probability Density Function of variations of three different backscatter characteristics measured over sand (blue) and seagrass (green) areas along two transects in Owen Anchorage: *E1*(top left panel), *SSCE* (top right panel), and *SSCI* (bottom panel).

MORINDA SHOAL - SBES DEPTH AND BACKSCATTER PARAMETERS

Fig. 15 shows the sea depth along the SBES transects over the Morinda Shoal survey area. Variations of the four measured backscatter characteristics *SSCE*, *E1*, *SSCI* and *EPW* along these transects and results of visual classification of the seafloor based on using video recordings are shown in Fig. 17.

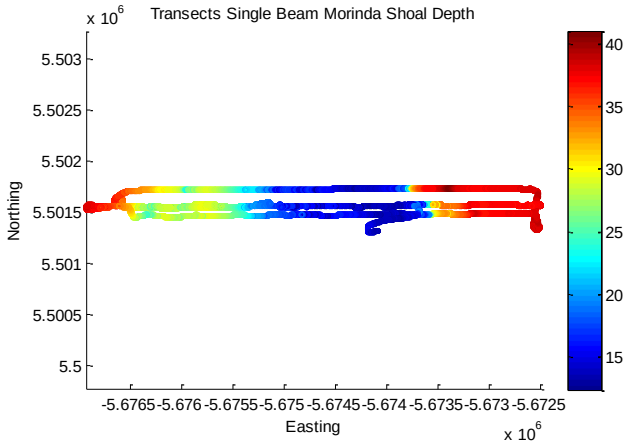

Fig. 15. Sea depth along SBES transects over the Morinda Shoal survey area.

Fig. 16. Video captures of three different seafloor types found in the Morinda Shoal area: Coral(left), Rock (middle) and Seagrass (right)

The probability density functions of the measured backscatter characteristic show obvious discrimination between three different habitats (Fig. 18). According to Fig. 18, the parameters of best seafloor discrimination are *SSCE* and *E1*. Three separate peaks can be easily distinguished in the PDFs of *SSCE* and *E1*, which are related to the three different type of bottom observed in the video footage taken along the transects in Morinda Shoal (Fig.16).

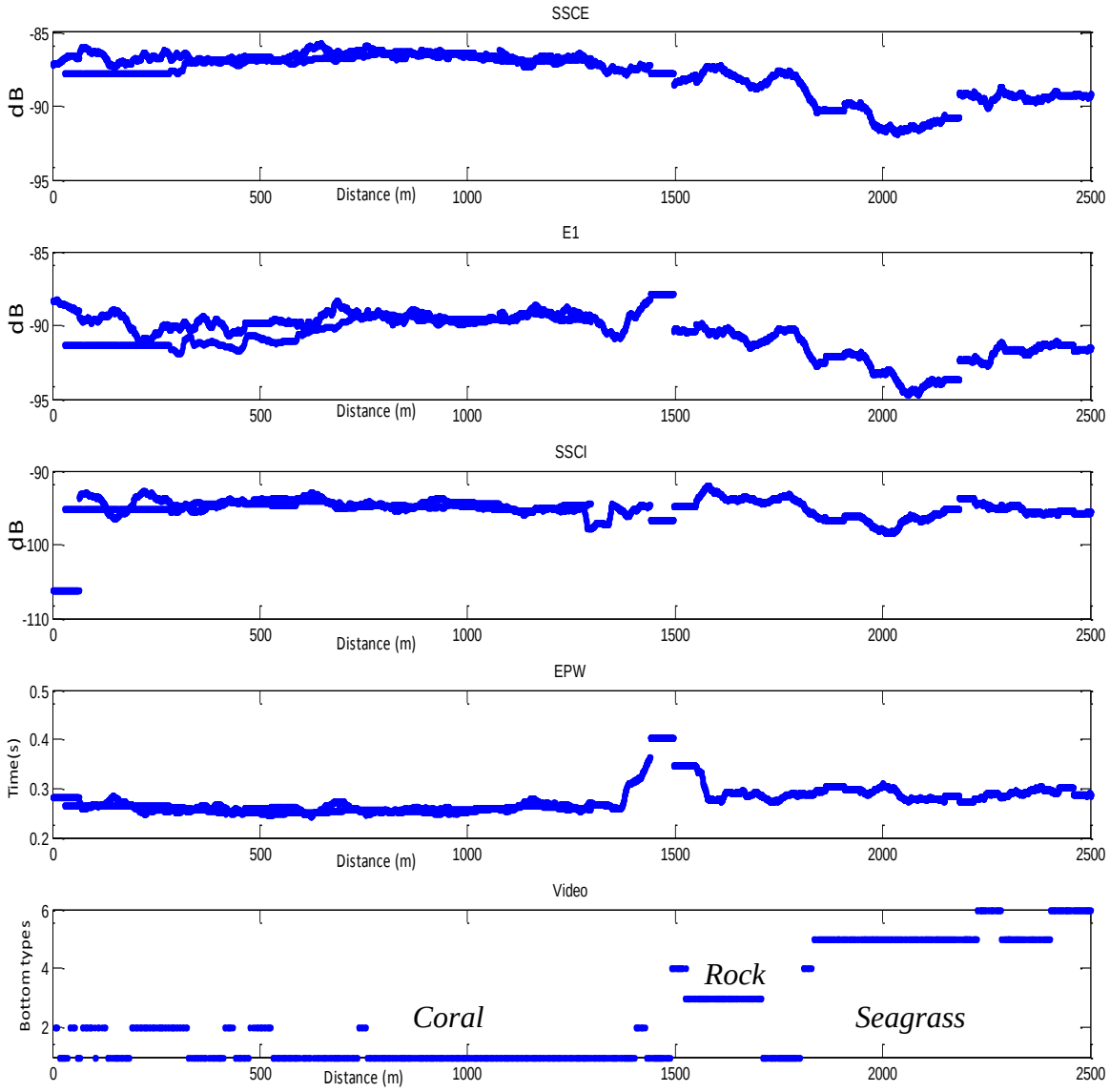

Fig. 17. Four different backscatter characteristics measured at 200 kHz along the SBES transects in Morinda Shoal (panels 1 to 4 from top: SSCE, E1, SSCI and EPW) and visual classification of the seafloor from video (bottom panel). The classification numbers correspond to different seafloor types as follows: 1 - Coral, 2. - Coral-Rock, 3 - Rock, 4 - Gravel, 5 - Seagrass (Low density), 6 - Seagrass (High density).

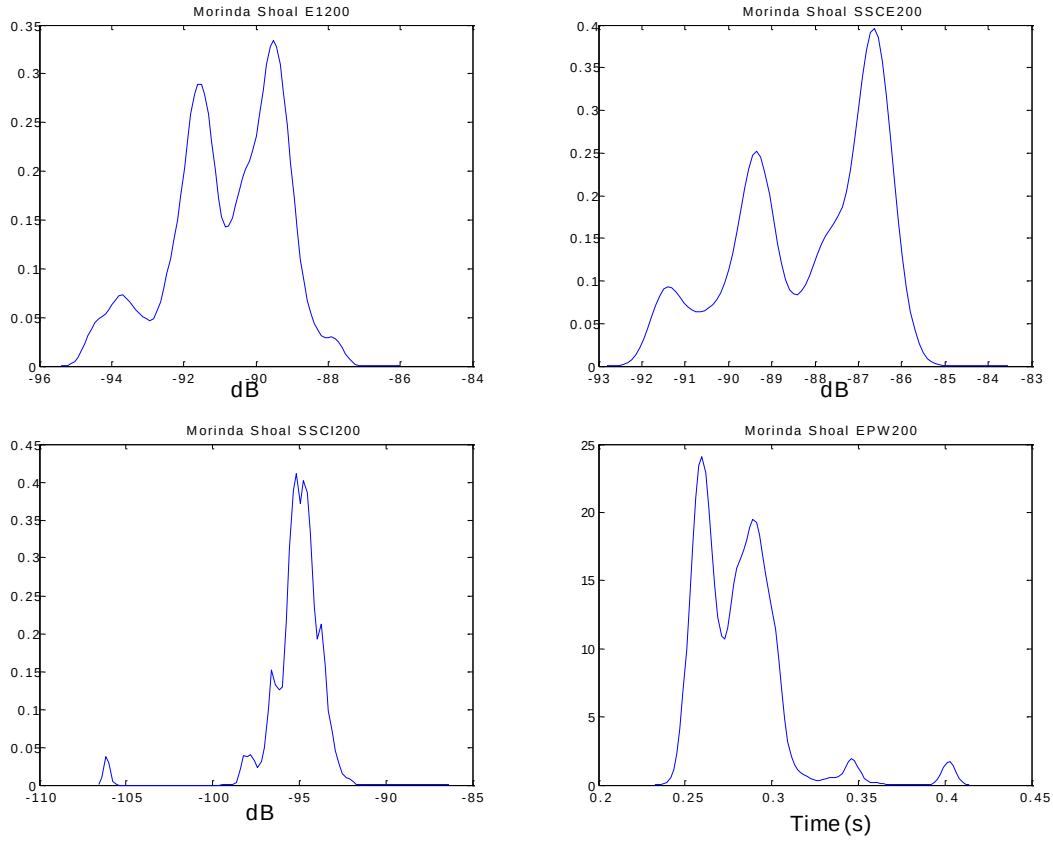

Fig. 18. Normalized distributions of four backscatter characteristics measured in Morinda Shoal: *E1*(top left), *SSCE* (top right), *SSCI* (bottomleft) and *EPW* (bottom right).

ANALYSIS OF THE DISTRIBUTION FUNCTION - OWEN ANCHORAGE

The PFA of the normalized backscatter intensity (SSCI) and energy (SSCE) for selected habitats is shown in Fig. 19 for 38 kHz (top panels) and 200 kHz (bottom panels). The aim of this analysis is to examine whether the scattering process is Gaussian or non-Gaussian. Gaussian scattering would cause variations of SSCE to be Gamma distributed and SSCI to be exponentially distributed. The PFA assesses the tail of a distribution, whereas PDFs assesses the shape of a distribution [21].

For the 38 kHz data from sand, the experimental distributions do not fit well any model distribution and seem to be closer to the Gamma distribution (Fig. 19 top). The distributions at 200 kHz can be reasonably well approximated by a Gamma model (Fig. 19 bottom)

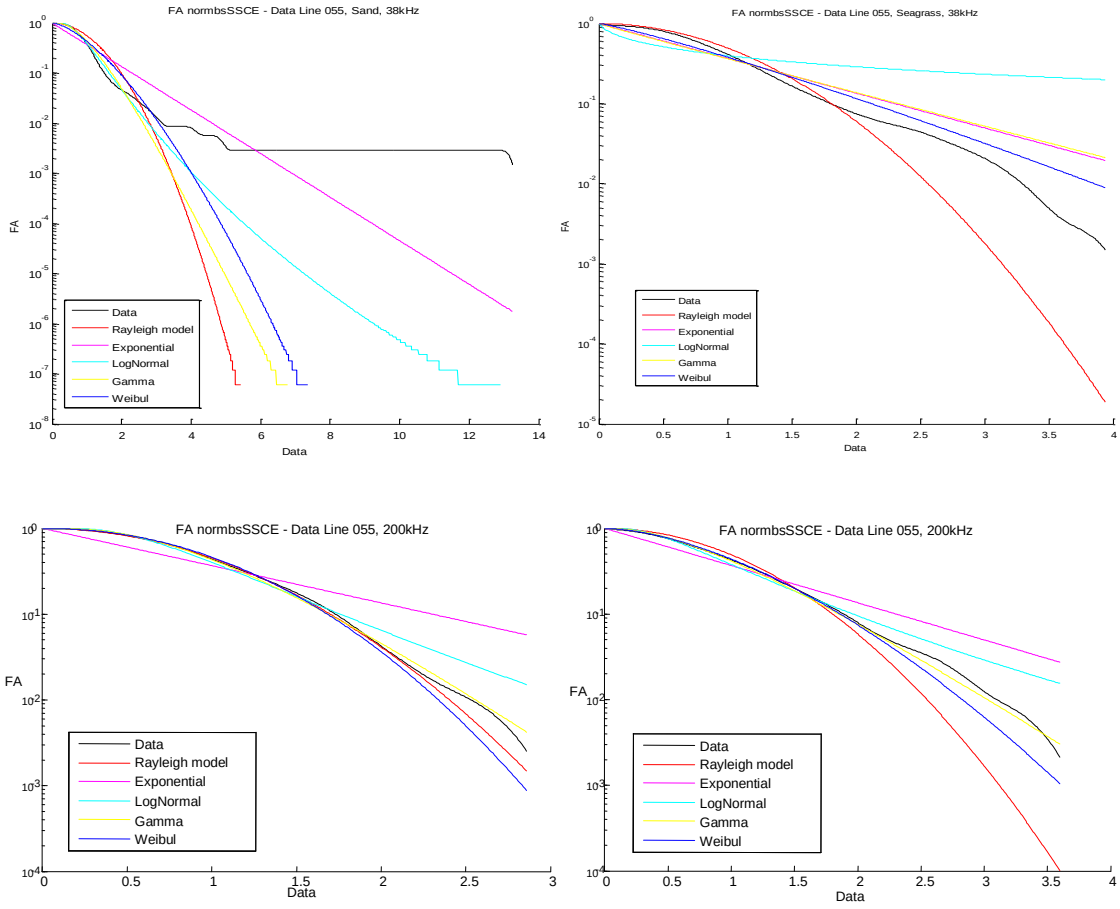

Fig. 19. PFAs of the SSCE backscatter characteristic measured from sand (left panels) and seagrass (right panels) at 38 kHz (top panels) and 200 kHz (bottom panels) in Owen Anchorage

4. CONCLUSIONS

The E1 and SSCE backscatter parameters measured at 200 kHz were the most robust for discriminating different seafloor habitats.

Seafloor classification based on these parameters was able to discriminate sand and seagrass in Owen Anchorage, and also more complex seafloor types, such as coral, found in Morinda Shoal.

Variations of the backscatter energy (SSCE) at 200 kHz observed from sand and seagrass were well approximated by the Gamma distribution, which suggests the scattering process to be nearly Gaussian.

V. TEMPORAL VARIABILITY OF SINGLE BEAM ECHO SOUNDER

1. INTRODUCTION

Previous studies [12][46] have shown that acoustic backscatter from seagrass is comparable to, or even stronger than that from surroundings areas of unvegetated seafloor. The physical mechanisms driving the higher backscatter from seagrass are poorly understood. Laboratory experiments have shown the sound speed in a plant-filled resonator to be dependent on plant biomass and tissue characteristics, which varies for different seagrass species [47]. In addition, the acoustic response from seagrass is influenced by photosynthetic activity which produces gas bubbles on the plants and in the water column [48]. However, it is unknown how much backscatter measured from seagrass is due to plant material, including air filled tissues, and how much of it might be due to microbubbles of gas produced by photosynthesis and/or respiration processes. If bubbles produced by gas emission are a significant contributor to the acoustic backscatter strength, then the backscatter intensity from seagrass could potentially change as the rate of gas production varies over the course of the day and season. Such variations, if they are significant, could seriously affect seagrass mapping by acoustic means. Gas bubbles released from seagrass due to photosynthesis and/or respiration are one of the most likely sources of strong scattering. If this is so, then the backscatter level from seagrass could vary with time, as the rate of gas emission changes during the day and in different seasons due to changes in the sun illumination. Using a *Simrad EQ60* single beam echosounder deployed from a jetty on Garden Island in Western Australia, acoustic backscatter from an area of dense seagrass *Posidonea* was measured at 38 kHz and 200 kHz every 2 s over 7 days. This study investigated the temporal variability of backscatter from an area of dense seagrass (Posidonia) measured at 38 kHz and 200 kHz using a single beam echosounder over a long time period (7 days).

2. METHODS

Acoustic backscatter from seagrass was measured between 2nd and 8th March 2010 using a dual-frequency *Simrad EQ60* single-beam echosounder, which was fixed to a jetty on Garden Island in Western Australia. The distance from the transducer head to the sediment-water interface was fixed at about 3.1 m over the whole measurement period. The transducer depth was about 1 m at the start of measurements and varied with tide by less than 1 m during the experiment. Backscatter echoes were collected every 2 s at both 38 and 200 kHz for seven days. The sonar pulse length was 512 μs at 38 kHz and 100 μs at 200 kHz.

The backscatter energy of the primary bottom echo and the instantaneous intensity at the bottom detection time were measured to analyse long-term variations and statistics of short-term fluctuations. The surface scattering coefficient was not calculated, because the echo sounder was not adequately calibrated with respect to transmitted power and receives gain. So, the backscatter intensity values are represented below in relative units. All sonar setting, such as transmitted power and pulse length were kept the same during the experiment to simplify comparison of backscatter measurements from seagrass and the surrounding areas of bare sediment.

Seagrass leaves are almost always moving under variable local currents due to tides and surface waves, which leads to significant and relatively fast fluctuations of the backscatter intensity measured from the same area of seagrass. A correlation analysis was used to select statistically independent samples of backscatter from seagrass for which the probability density function (PDF) and probability of false alarm (PFA) of backscatter characteristics were calculated and compared with the most typical statistical models associated with seafloor acoustic backscatter, such as Rayleigh, Gamma, K-distribution and lognormal models [49]

To compare backscatter from seagrass and bare sediments at the same frequencies, additional short-term measurements were made over an area of unvegetated muddy sand located about 10 m away from the seagrass measurement site at about the same sea depth.

3. BACKSCATTER FROM SEAGRASS AND ITS LONG-TERM VARIATIONS

0shows the level of backscatter intensity at 200 kHz and 38 kHz as a function of range from the sonar head to the bottom covered with seagrass and bare sand. Because the sea depth at the seagrass and sand sites was slightly different, the echoes from sand shown in 0 are aligned with those from seagrass at the bottom range.

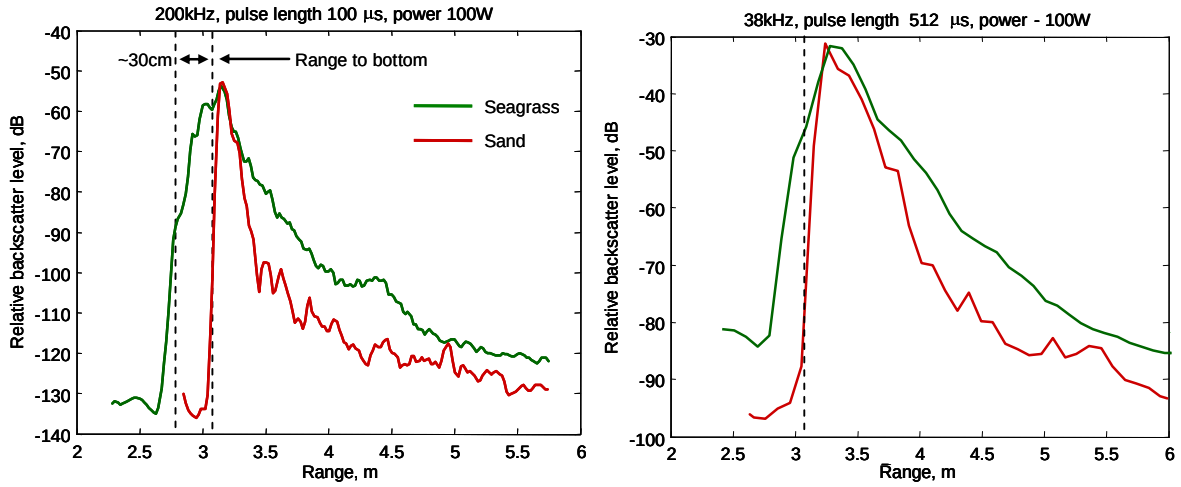

Fig. 20. Backscatter intensity level of the primary bottom echo from seagrass (green) and bare sand (red) averaged over 200 pings at 200 kHz (left) and 38 kHz (right).

The maximum amplitude of the mean envelope at 200 kHz is approximately the same for seagrass and sand. However, the backscatter signal recorded from the seagrass is stronger than bare sand both before and after the bottom detection range. The higher backscatter from the seagrass before the bottom detection point is the acoustic energy backscattered from the seagrass canopy and forms a less abrupt leading edge. The range to the leading edge of the echo from seagrass indicates that the canopy height was about 30 cm. The higher backscatter from seagrass (relative to bare sand) after the bottom detection point means that the backscatter strength of seagrass at oblique angles of incidence within the sonar beam is significantly stronger than that of bare sand. At 38 kHz, the effect of seagrass on backscatter echoes is similar but less pronounced.

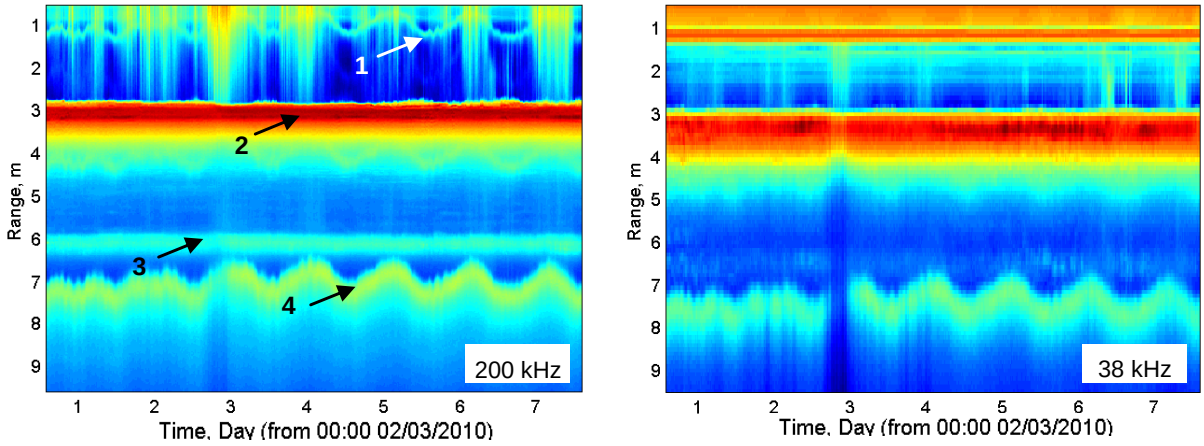

Fig. 21. Echograms from seagrass over 7 days of measurements at 200 kHz (left) and 38 kHz (right). Arrows with numbers in the top panel indicate echoes from different interfaces: 1- echo from the sea surface (received via the backward lobe of the sonar transducer); 2 – primary echo from the seafloor; 3 – secondary echo from the seafloor reflected by the sonar head; 4 – secondary echo from the seafloor reflected from the sea surface.

The echograms Fig. 21 show multiple echoes from different interfaces with the highest level of backscatter from the seafloor. The tidal variation of the sea depth is clearly seen in the varying arrival time of echoes reflected from the sea surface.

To analyse long-term variations of the acoustic backscatter strength of seagrass, the backscatter energy and intensity values were averaged over 200 sonar pings (400 s). Such averaging almost filtered out short-term fluctuations due to motion of seagrass leaves. Fig. 22 shows the variations of the backscatter level calculated for the average energy and intensity at 200 kHz and 38 kHz over 7 days of measurements. The variations of energy and intensity at 200 kHz were very small (less than 2 dB) and did not reveal any noticeable component of diurnal period. The energy of backscatter from the water column was also measured at the same time. For 200-kHz echoes, the water- column backscatter energy was calculated by integrating the backscatter intensity from 0.5 m to 2.5 m. A noticeable diurnal component with the maximum around midnight can be seen in the variations of water-column backscatter. The cause of such diurnal changes is not exactly known, but it is most likely associated with microorganisms (e.g. micro-algae, phytoplankton, etc.) residing in the water below the sea surface at night. Diurnal changes in the water-column backscatter at 200 kHz strength do not significantly affect backscatter from the seafloor.

Subtle diurnal variations of about 3 dB peak-to-peak can be seen in the seafloor backscatter at 38 kHz. These variations are negatively correlated with changes in the water-column backscatter, which

are, most likely, the major cause of seafloor backscatter variations at 38 kHz (in contrast to that at 200 kHz). The effect of water-column backscatter on the bottom echoes is clearly seen in Fig. 21. Strong water-column backscatter was observed right before midnight of day 3, which was probably caused by small fish schools appeared in the water at that time. This reduced considerably the energy of backscatter from the seafloor, especially at 38 kHz.

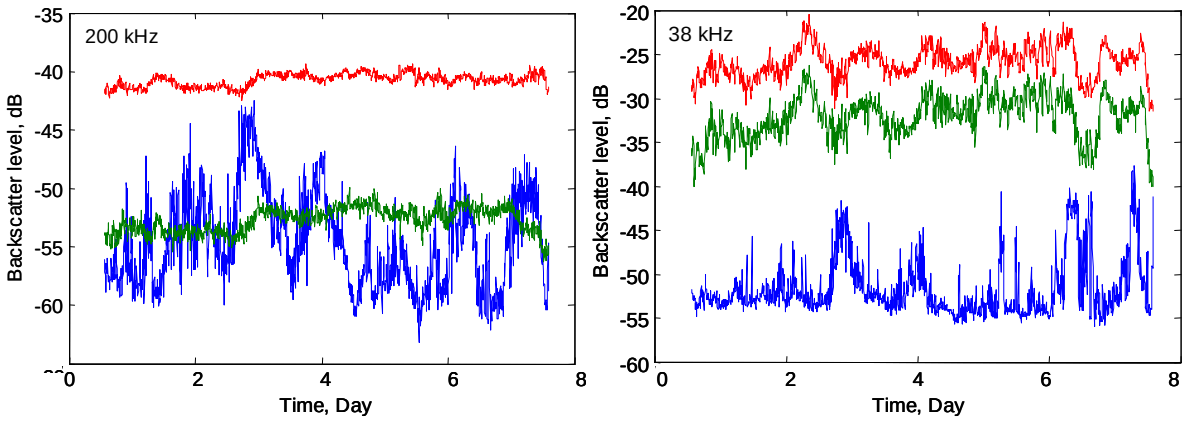

Fig. 22. Variations of backscatter energy (red) and instantaneous intensity (green) from seagrass and water-column backscatter energy (blue) observed at 200 kHz (left) and 38 kHz (right) over 7 days of measurements.

4. *STATISTICAL ANALYSIS OF SHORT-TERM FLUCTUATIONS*

To statistically analyse fluctuations of backscatter from seagrass, a data section of relatively stationary fluctuations during days 3 – 6 (about 170,000 pings) was chosen. An autocorrelation function of fluctuations was calculated at both frequencies to determine statistically independent samples of backscatter characteristics. It appeared that the 2-s ping interval was long enough for the adjacent samples of backscatter energy and intensity at 200 kHz not to be correlated, so that every sample could be taken for statistical analysis. At 38 kHz, adjacent samples were correlated to some extent, so every second sample was chosen for analysis.

A Probability Density Function (PDF) and Probability of False Alarm (PFA) were calculated for the distributions of backscatter energy and intensity at 200 kHz and 38 kHz. The experimental distributions of backscatter characteristics were compared with a number of model distributions which either had some physical ground for the measured backscatter parameters or provided reasonably good fits for backscatter data collected in previous experiments [21][49]. For the backscatter energy, the *K*-distribution, Gamma (Γ) and Lognormal models were tested, as the most appropriate ones. In addition,

an extreme value distribution model was tested for the backscatter energy data. It has been shown [50][51] that a sum of statistically independent backscatter intensity samples taken at different times of the backscatter signal tends to be Γ-distributed, if fluctuations of the backscatter envelop measured in different pings (from different scattering patches) have Rayleigh statistics (or an exponential distribution for intensity), i.e. when the backscatter process is Gaussian. A Γ-like distribution is also expected for the energy of processes that have other distributions of the instantaneous intensity, such as the *K*-distribution, with the tail shape similar to that of the exponential distribution. The echo signal from seagrass is relatively long for a short transmitted pulse of 100 μs (7.5 cm in terms of range resolution), so one can expect that backscatter samples taken from the same echo at different arrival times with intervals larger than 100 μs correspond to scattering from different parts (leaves and stems) of the seagrass canopy. Consequently, fluctuations of those samples should not be correlated and the variation of backscatter energy should tend to a Γ-like distribution.

The PDF and PFA of backscatter energy from seagrass are shown in Fig. 23. The Γ-distribution model fits the experimental PDF reasonably well, but the tail of the Γ-distribution is noticeably lighter than that of the experimental distribution, which is clearly seen in the PFA behaviour. The lognormal model provides a noticeably better fit for both most probable (i.e. PDF shape) and highest (i.e. PFA slope) values of backscatter energy. Although this does not have any reasonable physical explanation, some previous studies, e.g. [49][50], also showed a good fit of the lognormal model for backscatter energy fluctuations.

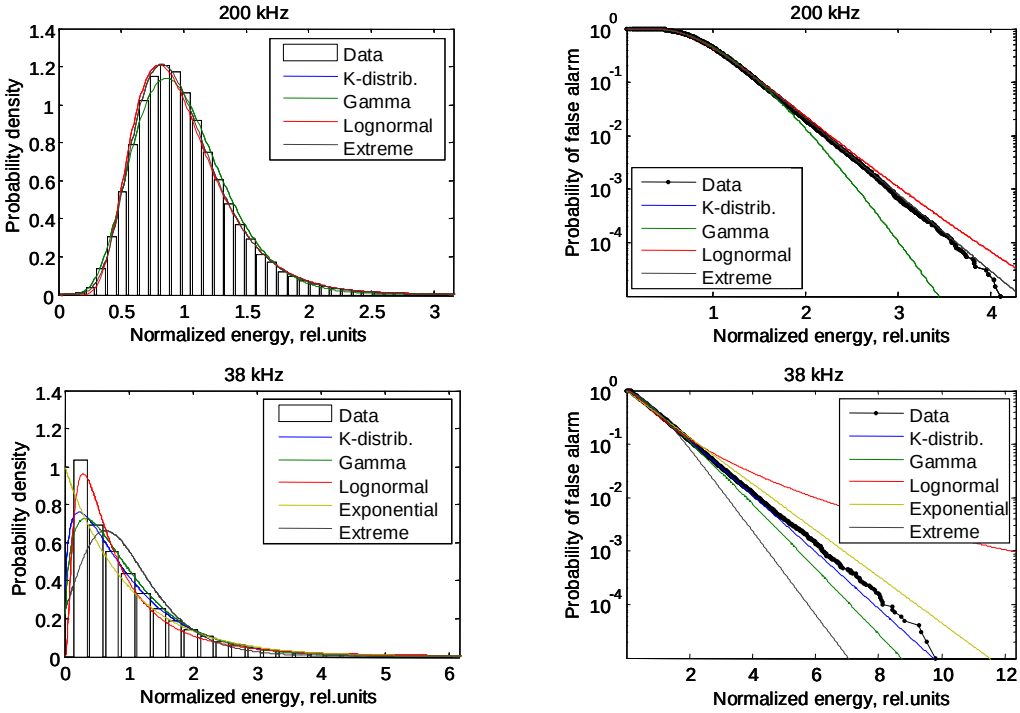

Fig. 23. Probability density function (left panels) and probability of false alarm (right panels) of backscatter energy fluctuations measured from seagrass at 200 kHz (top panels) and 38 kHz (bottom panels) shown with the best fits of different distribution models.

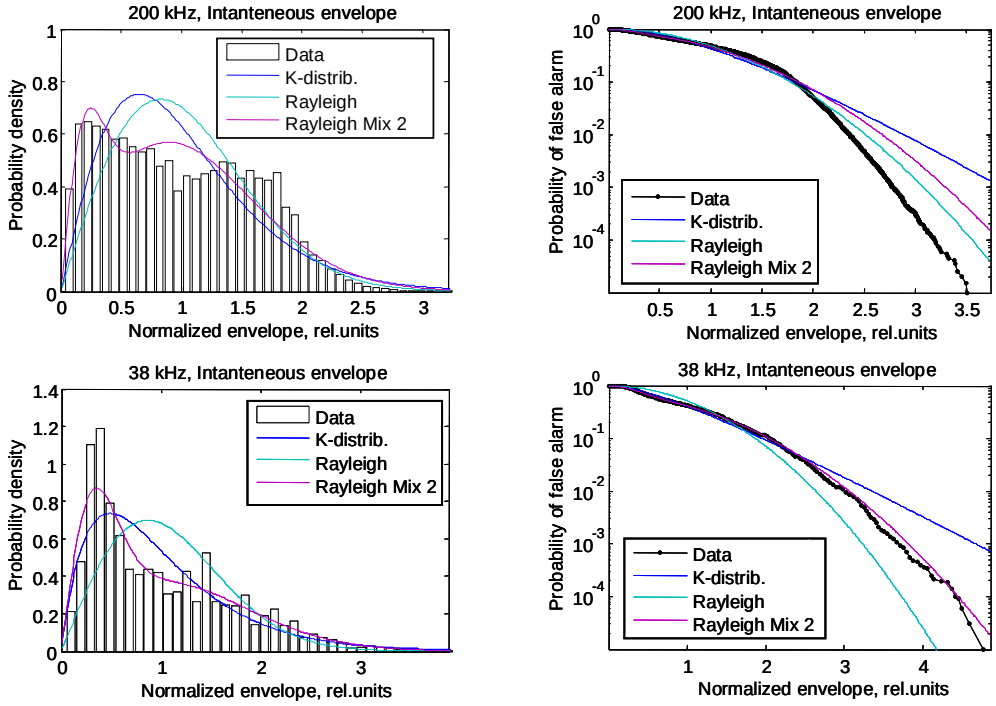

Fig. 24. Probability density function (left panels) and probability of false alarm (right panels) of instantaneous backscatter envelop from seagrass measured at the bottom detection time at 200 kHz (top panels) and 38 kHz (bottom panels) shown with the best fits of different distribution models.

Surprisingly, the extreme value distribution model provides the best approximation for the distribution of energy fluctuations, which also does not have any obvious physical explanation. The *K*-distribution model does not fit the experimental data at all and, hence it is not shown in this plot.

Statistics of short-term fluctuations of the backscatter energy from seagrass at 38 kHz is noticeably different from that at 200 kHz (Fig. 23). The experimental distribution can be reasonably well approximated by the exponential model, although the *K*-distribution model approximates slightly better the distribution tail. These two models provide a reasonable approximation because fluctuations of backscatter intensity samples taken at different times of the echo at 38 kHz are correlated with each in contrast to the echo at 200 kHz. In that case, the distribution of backscatter energy tends to be similar to the distribution of instantaneous backscatter intensity [50], which is either exponential for Gaussian processes with Rayleigh statistics of envelop fluctuations or *K*-distributed for non-Rayleigh processes.

If the backscatter process is Gaussian, i.e. the backscatter echo at every moment is a sum of signals backscattered from many different and statistically independent scatterers (e.g. facets of a rough surface or different patches within the scattering area), then the backscatter envelop should be Rayleigh distributed. When statistical parameter of such scatterers vary with range or time and the correlation length of those variations is comparable to the scattering area, the backscatter process becomes non-Gaussian and statistics of the backscatter envelop (square root of intensity) is non-Rayleigh. For such conditions, the *K*-distribution is often an appropriate model to describe fluctuations of the backscatter envelop [21]

The PDF and PFA of fluctuations of the instantaneous backscatter envelop measured at the bottom detection time are shown in Fig. 5. It is evident from the histograms of experimental data that the distribution of backscatter envelop is multimodal. At least two components can be distinguished in the PDF of backscatter envelop. Therefore, both Rayleigh and *K*-distribution models fail in approximating the experimental distribution. A two-component Rayleigh mixture distribution approximates quite well both PDF and PFA of the backscatter envelop at 38 kHz. This means that the backscatter from seagrass at this frequency can be represented by a superposition of two independent Gaussian processes of different characteristics, which could be scattering from the seagrass canopy and from the underlying sediment. The second component is affected by randomly varying sound attenuation in the canopy.

In contrast to echoes at 38 kHz, the maximum likelihood estimator could not find parameters of the two-component Rayleigh model satisfactorily fit the distribution of envelop at 200 kHz. This might be due to individual components of the multimode distribution, which are non-Rayleigh in this case. Perhaps, more complex models are needed to approximate such kind of distributions.

The distribution models which provide the best fit for the experimental data are summarized in Table 2.

	38 kHz	200 kHz
Energy	*K*-distribution	Extreme value and Gamma
Instantaneous Envelope	2-component Rayleigh mixture	Multimode distribution of uncertain components

Table 2. Distribution models found to fit the experimental data from seafloor backscatter collected over seagrass.

5. CONCLUSIONS

The experiment showed that the backscatter strength from seagrass at vertical incidence at moderate (38 kHz) and high (200 kHz) frequencies is comparable to that from the bare sediment (muddy sand). However, the backscatter echo from seagrass is noticeably longer than that from sand, which is due to the greater contribution of the acoustic energy backscattered at angle different from vertical. Consequently, the total energy backscattered from the seagrass canopy is higher than that from sand.

The backscatter data collected over seven days from the same area of seagrass using a fixed single-beam echosounder did not reveal any significant long-term variations including those of diurnal period. This is a somewhat unexpected result, because the main cause of stronger backscatter from seagrass was believed to be gas bubbles produced in leaves by photosynthesis, which should vanish or be much less active at the night time. Some small variations of a diurnal period were observed in the backscatter intensity at 38 kHz. However, these variations are most likely due to diurnal changes in the backscatter from the water column, rather than changes in the scattering properties of seagrass. Water-column scattering increases the transmission loss of sonar signals propagated to the seafloor and scattered back to the sonar transducer. This effect is more significant at a lower frequency of 38 kHz.

Seagrass leaves are usually moving under variable local currents. This motion leads to short-term random fluctuations of backscatter from seagrass. Statistics of backscatter energy fluctuations at 200 kHz can be roughly described by a Γ-distribution model, which is expected for a sum of statistically independent processes with Rayleigh-like statistics. Fluctuations of individual samples of the echo signals from the seafloor at 38 kHz are partly correlated with each other. This results in the distribution shape to be somewhat similar to that of the exponential distribution of backscatter envelop typical for a single Gaussian process, although the *K*-distribution model provides the best fit for the energy at 38 kHz.

Statistics of the instantaneous backscatter envelop is more complex. The histograms of fluctuations reveal obvious multimode distributions, which can be well approximated at 38 kHz by a two-component Rayleigh mixture model. However, at 200 kHz this kind of model cannot fit the experimental distribution.

VI. CONCLUSIONS

The objectives of this project were two-fold: 1) first, to evaluate different seafloor backscatter parameters from processed SBES data in order to determine which is the most informative for habitat mapping, and 2) to examine the temporal variation of backscatter from a vegetated seafloor and find out if there are significant changes due to diurnal changes in the sun illumination and photosynthesis rate.

To address the first objective, this dissertation has analysed the properties of the echoes recorded using the Single Beam echo sounder (SimradEQ60) to find out the best discriminator for high-frequency acoustic classification of seafloor habitats. Echoes from different types of seafloor, including bare and vegetated seafloors, were studied using the backscatter energy, intensity and the energy of the echo tail (E1) at different sonar frequencies (38 kHz and 200 kHz). The most robust backscatter parameters for seafloor classification using SBES were found to be the energy of the whole echo and its tail. These parameters were able to distinguish seagrass meadows on bare seafloor wherever the bottom is flat and the vegetation patches are of moderate to high density.

The modelling study evaluated the dependence of SBES backscatter characteristics on sea depth, the seafloor backscatter coefficient and the transmitted pulse width. The E1 parameter was found to be depth dependent, because this parameter was changing with the insonification area within the sonar beam. A more accurate calculation of the seafloor insonification area, which corresponds to the echo tail, along with an appropriate correction of the E1 estimate for this area reduced considerably the depth dependence of this backscatter characteristic.

This study addressed the question of whether the high frequency acoustic backscatter from seagrass varied significantly with time or not. This was carried out by studying backscatter variations measured from seabed vegetation over a long time period of 7 days. The results obtained in this study found that the diurnal variation in light, which should cause changes in the photosynthesis of the seagrass, does not seem to significantly influence the received backscatter signal at both frequencies of 38 kHz and 200 kHz. Some small variations of a diurnal period were observed in the backscatter intensity at 38 kHz. However, these variations were most likely due to diurnal changes in the backscatter from the water column, rather than changes in the scattering properties of seagrass.

FUTURE WORK

More comprehensive measurements are needed to further understand the physics of acoustic backscatter from seagrass. Such measurements should be made over different areas and types of seagrass, over longer time periods and, preferably, in different seasons. Moreover, visual observations of gas bubble emission and physical samples of seagrass tissue should be taken to measure its gas content in parallel to acoustic measurements.

ACKNOWLEDGMENT

The author would like to thank the CMST group for their help with this study. Especially to Dr. Alexander Gavrilov and Dr. Iain M. Parnum for their excellent supervision in the project, their participation and patience in instructing the author in the subject.

BIBLIOGRAPHY

[1] *Monitoring for action: Understanding Western Australia's changing marine and coastal environments* 24 November 2009. Symposium. **15**

[2] Hemminga, M. A., and C. M. Duarte, *Seagrass ecology***,** 2000, Cambridge University Press. 17

[3] Nupur M. Smith, Diana I. Walker, *Canopy structure and pollination biology of the seagrasses Posidonia australis and P. sinuosa,* 2002, University of Western Australia, ELSEVIER (Aquatic Botany).

[4] Environment & Infrastructure Pty Ltd, *Cockburn Sound Management Council. The state of Cockburn Sound. A pressure-State-Response Report.*

[5] A.Siccardi, R.Bozzano, *A test at sea for measuring acoustic backscatter from marine vegetation,* 1998, Institute for Naval Automation, CNR, Italy.

[6] Evgeni L. Shenderov, *Some physical models for estimating scattering of underwater sound by algae*, 1998, Research and Development Institute "Morfizpribor", J. Acoust. Soc. Am.

[7] Iain M. Parnum, *Benthic Habitat Maping using MultiBeam Sonar Systems,* 2007, Curtin University.

[8] Yao-Ting Tseng*, Recognition and assessment of seafloor vegetation using a Single Beam Echosounder*, 2009, Curtin University.

[9] V.A.I. Huvenne, Ph. Blondel, J.-P. Henriet, *Textural analyses of sidescan sonar imagery from two mound provinces in the Porcupine Seabight*, 2002, University of Bath, ELSEVIER (Marine Geology)

[10] Timothy C. Gallaudet and Christian P. de Moustier, *High-frequency volume and boundary acoustic backscatter fluctuations in shallow water,* 2003, Marine Physical Lab, Scripps Institution of Oceanography, J.ACOUSTIC.

[11] A. Fornes, G. Basterretxea, A. Orfila, A. Jordi, A. Alvarez, J. Tintore, *Mapping Posidonia oceanica from IKONOS*, 2006, ELSEVIER (Photogrammetry & remote sensing).

[12] Jaraslaw Tegowski, Natalia Gorska, Zygmunt Klusek, *Statistical analysis of acoustic echoes from underwater meadows in the eutrophic Puck Bay (Southern Baltic Sea),* Institute of Ocenanology, Polish Academy of Sciences, 2003, ELSEVIER (Aquatic Living Resources)

[13] L.J. Hamilton, *Acoustic Seabed Classification Systems, Maritime Operations Division. Aeronautical and Maritime Research Laboratory*, 2001, Defence Science and Technology Organisation (Australia).

[14] Herman Medwin and colleagues, *Sounds in the Sea. From Ocean Acoustics to Acoustical Oceanography*, 2005, Cambridge University Press.

[15] Xavier Lurton, *An Introduction to Underwater Acoustics. Principles and Applications,* 2002, Springer.

[16] Richard O. Duda, Peter E. Hart, David G. StorkA Wiley, *Pattern classification. Second Edition*, Interscience Publication. John Wiley & Sons, inc.

[17] J. D. Penrose, P. J. W. Siwabessy, A. N. Gavrilov, I. M. Parnum, L. J. Hamilton, A. Bickers, B. Brooke, D. A. Ryan and P. Kennedy, *Acoustic Techniques for Seabed Classification*, 2005, CRC.

[18] Philippe Blondel, *A review of acoustic techniques for habitat mapping,* Department of Physics, University of Bath, Claverton Down, Bath BA2 7AY, UK.

[19] Fortin, Marie-Josée; Dale, Mark, *Spatial Analysis: A guide for ecologists,* 2005, Cambridge University Press.

[20] Jason Owen, Petra Kuhnert & Bill Venables, David Rossiter, J H Maindonald, *Geographic Data Analysis Using R, An Introduction to R, Software for Statistical Modelling & Computing, The R Guide,* 2008.

[21] Anthony P. Lyonsa and Douglas A. Abrahamb, *Statistical characterization of high-frequency shallow-water seafloor backscatter,* 1997, publication 1999, SACLANT Undersea Research Centre, J.ACOUSTIC.

[22] Norm Campbell, Peter Caccetta and Jared O'Connell (CSIRO Mathematical & Information Sciences, Floreat WA); Iain Parnum (CMST, Curtin University, Bentley WA); Paul Kennedy (Fugro Technical Services, Balcatta WA); and John Keesing and Tennille Irvine (CSIRO Marine & Atmospheric Research, Floreat WA*), Posterior Probability Images Incorporating the Backscatter Angular Response for Multibeam Data*

[23] V.A.I. Huvenne, Ph. Blondel, J.-P. *Textural analyses of sidescan sonar imagery from two mound provinces in the Porcupine Seabight,* 2002, Henriet, University of Bath, ELSEVIER (Marine Geology)

[24] G.Canepa, N.G.Pace. Undersea Research Centre, *Seafloor segmentation from multibeam bathymetric sonar,* ECUA 2000, Italy.

[25] DAL & ENGINEERING PTY LTD, *Benthic habitat mapping for 2002 of selected areas of Cockburn sound*

[26] K.W.Holmes, K.P.Van Niel, G.A.Kendrick, B.Radford, *Probabilistic large-area mapping of seagrass species distributions,* 2005, CRC, University Western Australia.

[27] Paulus Justiananda Wisatadjaja Siwabessy, *An investigation of the relationship between seabed type and benthic and bentho-pelagic biota using acoustic techniques,* School of Applied Science 2001

[28] Iain Parnum. Centre for Marine Science and Technology, *Processing Single Beam Sonar data from Ningaloo Marine Park,* 2009, Australian Institute of Marine Science.

[29] J. Burczynski. Centro de Entrenamiento Acústico, *Introduccion al uso de sistemas sonar para la estimacion de la biomasa de peces,* Noruega, 1982, IMARPE, Lima, Perú.

[30] Brandt Tso and Paul M. Mather, *Classification Methods for remotely sensed data,* Published 2001 by Taylor and Francis.

[31] Frederick T. Short, Hilary A. Neckles. Department of Natural Resources, *The effects of global climate change on seagrasses* , USA 1998, University of New Hampshire, ELSEVEIR (Acoustic Botanic)

[32] Peter A. Burrough and Rachel A. McDonnell, *Principles of Geographical Information Systems. Spatial Information Systems and Geostatics,* 1998, Oxford University Press.

[33] J.-P. Hermand, Environmental Hydroacoustics, Dept. of Optics and Acoustics. Université Libre de Bruxelles, *J.-P. Hermand, Environmental Hydroacoustics, Dept. of Optics and Acoustics. Université Libre de Bruxelles,* IEEE.

[34] Applied Physics Laboratory. University of Washington. Seattle, *APL-UW High-frequency. Ocean Environmental Acoustic models handbook,* 1994, Technical Report.

[35] Darrel R. Jackson, Michael D. Richardson, *High-Frequency Seafloor Acoustics. Monograph series in underwater acoustics,* Sprinter ed. 2007

[36] The University of Queensland, Australia, *Distribution of seagrass in Moreton Bay,Results from Dennison et al*. 1998

[37] Azriel Rosenfeld and Larry S. Davis, *Image Segmentation and Image Models*, IEEE, vol. 67, nº.5, may 1979.

[38] Guy B. Coleman and Harry C. Andrews, *Image segmentation by Clustering,* IEEE, vol. 67, nº.5, may 1979.

[39] W. John Richardson, Charles R. Greene, Jr., Charles I. Malme, Denis H. Thomson, *Marine Mammals and Noise,* Academic Press (AP). 1995.

[40] Alexander N. Gavrilov and Iain M. Parnum, *Fluctuations of Seafloor Backscatter Data from Multibeam Sonar Systems*, IEEE jounal of oceanic engineering. 2010.

[41] Brian R. La Cour, *Statistical characterization of active sonar reverberation using Extreme Value Theory*, IEEE journal of oceanic engineering, vol.29, n2, April 2004.

[42] Noela Sanchez-Carnero, Cristina Bernandez, Marek Moszynki & Juan Freire, *Development o fan open approach for acoustic marine benthic habitat classification,* 2nd International Conference & Exhibition on "Underwater Acoustic Measurements: Technologies & Results"

[43] J.-P. Hermand, *Photosyntesis of Seagrass Observed In Situ from Acoustic Measurements,* 2004 IEEE.

[44] C. S. Clay and H. Medwin, *Acoustical Oceanography: Principles and Applications*, New York: Wiley, 1977.

[45] Alexander Gavrilov, L-3 Communications Nautronix, *SML Sonar Interference Analysis: Phase 2B*, Curtin University, Centre for Marine Science and Technology, 2008.

[46] I. Parnum, A. Gavrilov and J. Siwabessy, "Analysis of multibeam sonar data for the purposes of seabed classification". In *Proc. Underwater Acoustic Measurements: Technologies & Results, 2nd International Conference and Exhibition*, Heraklion, Crete (2007)

[47] P.S. Wilson and K.H. Dunton, "Laboratory investigation of the acoustic response of seagrass tissue in the frequency band 0.5-2.5 kHz", *J. Acoust. Soc. Am.,* v.125(4), pp.1951-1959 (2009)

[48] J.-P. Hermand, P. Nascetti, and F. Cinelli, "Inversion of acoustic waveguide propagation features to measure oxygen synthesis by Posidonia oceanica," in *Proceedings of the Oceans **'98** IEEE/OES Conference* (C. 0. Committee, ed.), vol. II, (P iscataway, NJ), pp. 919-926 (1998).

[49] T.C. Gallaudet and C.P. de Moustier, "High-frequency volume and boundary acoustic backscatter fluctuations in shallow water", *J. Acoust. Soc. Am.,* v. 114 (2) (2003)

[50] A. Gavrilov and I. Parnum, "Fluctuations of seafloor backscatter data from multibeam sonar systems", *IEEE J. Ocean. Eng.,* vol.35, issue 2, pp. 209-219 (2010)

[51] D. Middleton, "New physical–statistical methods and models for clutter and reverberation: the *KA*-distribution and related probability structures", *IEEE J. Oceanic Eng.*, vol. 24, no. 3, pp. 261-284 (1999)

APPENDIX:

TECHNICAL REPORT – EXPERIMENTAL DATA SEAGRASS TIME DEPENDENCE

EXPERIMENTAL PROCESS FROM THE SINGLE BEAM EQ60 – JETTY FREMANTLE

SAND	38kHz	200 kHz
Date	Start: 16:30h, 25/01/2010 25.3º Finish: 15:45h, 27/01/2010	
Predicted Tide Hire	25/01/2010 – 17:36h → 1.02 26/01/2010 – 04:18h → 0.38 18:33h → 1.08 27/01/2010 – 04:41h → 0.33 19:27h → 1.13	
File	L0004 (Total No. files = 129)	
Power	100W	100W
Pulse Length	0.256ms	0.100ms
Ping rate	2s	
Echogram diagram	Gain Fish Purse seine Ping filter Surface-manual	

SAND (Settings variations)	File	38kHz [µs]	200 kHz [µs]
Ping rate = 0.5s	L006	4096	1024
	L007	2048	512
	L008	1024	256
	L009	512	128
	L010	256	100

SAND (Settings variations)	File	Inclination [cm]	Inclination [º]
	L011	13.5	30
	L012	9	21
	L013	4.5	11
	L014	22-26	43-48

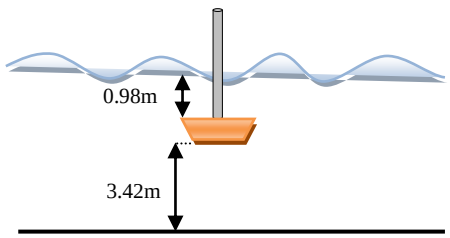

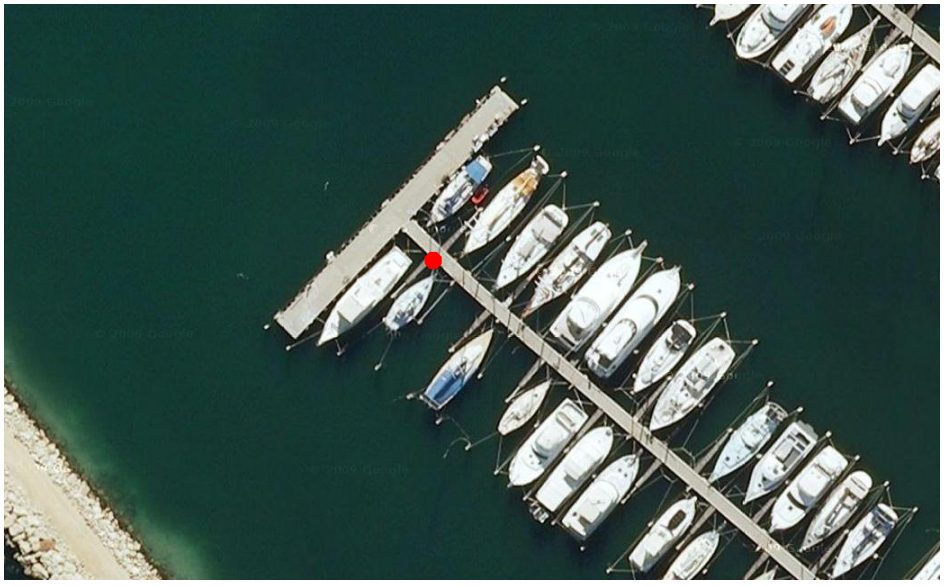

Transducer position in the jetty of Fremantle (red spot)

Aerial photography of the Fremantle dock

EXPERIMENTAL PROCESS FROM THE SINGLE BEAM EQ60 – NAVY HMAS STIRLIN, *PERTH.*

SEAGRASS	**38kHz**	**200 kHz**
Date	**Start[2]: 13:26, 02/03/2010 24.6º Finish: 09/03/2010**	
Predicted Tide Height	**02/03/2010 – 05:06h → +0.5 L 11:22h → +0.7 H 17:12h → +0.5 L 23:19h → +0.6 H 03/03/2010 – 04:43h → +0.5 L 11:34h → +0.7 H 18:32h → +0.5 L 23:24h → +0.6 H 04/03/2010– 04:13h → +0.5 L 11:52h → +0.8 H 05/03/2010– 03:43h → +0.4 L 12:16h → +0.8 H 06/03/2010– 03:22h → +0.4 L 12:48h → +0.8 H 07/03/2010– 03:27h → +0.3 L 13:29h → +0.8 H 08/03/2010– 03:42h → +0.3 L 14:28h → +0.8 H 09/03/2010– 03:55h → +0.3 L 16:02h → +0.8 H**	
Test File	**L0016**	
File	**L0017 (Total No. files = 459)**	
Power	**100W**	**100W**
Pulse Length	**0.512ms**	**0.100ms**
Ping rate	**2s**	
Echogram diagram	**Gain Fish Purse seine Ping filter Surface-manual**	

[2] **The data was checked the 04/03/2010 approximately from 01:30 till 03:00pm and everything was all right. An underwater video camera was set up at this time, recording during 8h the insonification area.**

Seagrass(Settings variations[3])	File	38kHz [µs]	200 kHz [µs]
Height (the same as for	L0018	Change power Low → High	
L0017)	L0019	1024	256
3.12m	L0020	2048	512
	L0021	4096	1024
New Height	L0022	256	100
Pole was moved around	L0023	512	100
4.09m	L0024	512	100
	L0025	1024	256
	L0026	2048	512
	L0027	4096	1024
Original Position	L0028	4096	1024
2.14m	L0029	256	100
	L0030	512	256
	L0031	1024	512
	L0032	4096	1024

SAND	File	38kHz [µs]	200 kHz [µs]
Bare Seafloor	L0033	256	100
Lowest Power	L0034	512	256
4.61m	L0035	1024	512
	L0036	4096	1024
3.64m	L0037	256	100
	L0038	512	256
	L0039	4096	1024
2.66m	L0040	256	100
	L0041	4096	1024

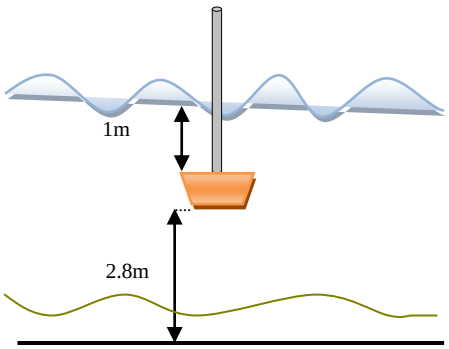

[3] **Ping rate 0.5 s for files L0018 to L0041.**

Transducer position in the jetty in Garden Island (red spot seagrass, yellow sand)

Aerial photography of Garden Island